THESIS - KI142502

SENSOR FUSION AND TEMPORAL INTEGRATION FOR TOUCH INTERFACE INDOOR POSITIONING

Hani Ramadhan
5113201907

ADVISOR

Charles LENAY
Dominique LENNE

MAGISTER PROGRAM
DEPARTMENT OF INFORMATICS ENGINEERING
FACULTY OF INFORMATION TECHNOLOGY
INSTITUT TEKNOLOGI SEPULUH NOPEMBER
SURABAYA
2016

[This page is intentionally left blank]

Thesis Recommendation Form

This thesis is submitted as a requirement for Magister Komputer (M.Kom) degree completion

at

Institut Teknologi Sepuluh Nopember

By:

Hani Ramadhan

ID: 5113201907

Presentation date: 10th July 2015

Graduation Period: March 2016

Approved by

Postgraduate Program Director

Prof.Ir. Djauhar Manfaat, M.Sc, Ph.D

NIP. 19601202 198701 1 001

Abstrak

Dalam kunjungan wisata atau budaya, panduan terhadap objek menarik sangat berguna untuk menambah pengetahuan dan pengalaman pengunjung di lokasi tersebut. Dewasa ini, dengan bantuan teknologi modern, aplikasi bergerak mampu menjadi pemandu wisata mandiri otomatis dengan sistem sadar konteks. Kebanyakan, unsur konteks yang digunakan dalam aplikasi-aplikasi ini adalah posisi dua dimensi (2D). Meskipun begitu, ada beberapa kemungkinan lain agar tiap unsur konteks dari perangkat pintar ini dapat diteliti lebih lanjut.

Berkat sensor dari ponsel pintar, konteks-konteks tersebut, yang terdiri dari konteks dalam 3 dimensi (3D) dari posisi dan orientasi (dalam sumbu X, Y, dan Z), dapat ditangkap oleh ponsel pintar. Dimensi-dimensi ini akan diteliti untuk mendapatkan kemungkinan keberhasilan digunakannya ponsel pintar yang digenggam sebagai *pointer* terhadap objek menarik. Hal ini dilakukan karena posisi 2D tidak bisa menangani konteks ketinggian. Sehingga, pengalaman pengguna dapat ditingkatkan karena mereka tidak terhalang secara visual dan audio. Tetapi, sensor-sensor ini memiliki galat pengukuran yang tinggi. Sehingga, suatu penggabungan sensor diterapkan untuk menangani galat tersebut.

Penelitian ini menerapkan metode untuk memperkirakan orientasi sudut dan posisi dengan berbagai *filter*, yakni Complementary Filter dan Kalman Filter. Complementary Filter melibatkan *gyroscope*, *magnetometer*, dan *accelerometer* dari sensor inersial ponsel pintar. Sedangkan, Kalman Filter melibatkan *accelerometer* dan hasil *Wi-Fi fingerprinting* yang didapatkan dari pengamatan lingkungan. Evaluasi perkiraan-perkiraan hasil penggabungan observasi sensor oleh *filter-filter* tersebut menggunakan ilustrasi grafis dan evaluasi statistika untuk mengukur kualitas reduksi galat dari tiap *filter*.

Hasil dari performa *filter* menunjukkan bahwa kualitas perkiraan orientasi oleh *Complementary Filter* cukup baik untuk menghasilkan sudut yang sesuai. Namun, perkiraan posisi oleh *Kalman Filter* menunjukkan hasil yang kurang baik akibat integrasi ganda terhadap derau dan pengaruh besar *Wi-Fi fingerprinting*. Hasil *Wi-Fi fingerprinting* menunjukkan perkiraan posisi yang tidak akurat. Hal ini menunjukkan bahwa perkiraan posisi tidak dapat digunakan dalam penelitian ini. Sedangkan, dalam percobaan menunjuk objek di laboratorium, perkiraan orientasi sudut memberikan hasl yang cukup baik dengan ponsel pintar.

Secara ringkas, perkiraan posisi dan orientasi 3D dengan *Complementary Filter* dan *Kalman Filter* dalam ponsel untuk *pointer* tidak dapat digunakan

menurut penelitian ini. Meskipun begitu, masih perlu diteliti mengenai penerapan *filter* lainnya untuk perkiraan posisi dan observasi lain untuk membantu perkiraan yang baik. Walaupun penggunaan *filter* dan observasi lain dapat mengorbankan sumber daya dari ponsel pintar.

Kata kunci: *Context-aware systems*, *Indoor positioning*, *Wi-Fi fingerprinting*, *sensor fusion*

Summary

During cultural or tourism visits, a guide of the interesting objects is useful to enhance the knowledge and the experience of the visitors. Nowadays, because of the modern technologies, mobile applications are capable to be a personal autonomous guide in the case of context-aware system. Mostly, the context element used in these applications is the position in two dimension (2D). However, there are more possibilities using the context elements from smartphone that can be explored.

Thanks to smartphone sensors, the contexts which can be captured by smartphone are composed in 3 dimensions (3D) of both position and orientation (in X, Y, and Z axes). Those dimensions are used to explore the feasibility of smartphone which can held by hand as pointer to interesting objects, which can't be handled by 2D position only. Thus, the user experience can be enhanced, as they don't get vision-blocked or audio-blocked. However, those sensors have erroneous measurements. Hence, a sensor fusion is applied to overcome this drawback.

The sensor fusion can be implemented not only using the internal smartphone sensors, but also the external environment. In this case of indoor environment, the Wi-Fi fingerprinting approach, which widely used as indoor positioning algorithm, can be considered as external observation. Even though so, the quality of the fusion should be studied to assure that it is feasible to use smartphone a pointing device in indoor environment.

This study proposed a method to estimate orientation and position using different filters, namely Complementary Filter and Kalman Filter respectively. The complementary filter involves the gyroscope, magnetometer, and accelerometer from the smartphone inertial navigation sensors, while the Kalman Filter involves accelerometer and the Wi-Fi fingerprinting result which come from environmental measurement. To evaluate these estimations, the graphical representation and statistical evaluation are used to measure the filters' quality in reducing the errors.

The results of the filters' performance showed that orientation estimation was adequate to give acceptable angle. But, unfortunately, position estimation had resulted in poor performance because of the double integration toward noise and the heavy influence from Wi-Fi fingerprinting. The Wi-Fi fingerprinting resulted inaccurate positioning. This concluded that the position estimation cannot be used at all in this study. In laboratory object pointing field experiment, the orientation estimation gave passable estimation to locate an object by a fixed smartphone position.

To sum up, the 3D position and orientation estimation using Complementary Filter and Kalman Filter might not be feasible according to this study. However, regarding to 3D position estimation, possibly there are other methods than Kalman Filter which might be used as state estimator. And also, there are various external measurements which might help to achieve better estimation. Although, the drawbacks between the more sophisticated methods and the computation power and capability of smartphone should be considered for a good user experience.

Keywords: Context-aware systems, Indoor localization, Wi-Fi fingerprinting, sensor fusion

Résumé

Pendant une visite culturelle ou touristique, un guide des objets intéressants est utile pour améliorer la connaissance et l'expérience des visiteurs. Actuellement, des applications mobiles sont capables de devenir des guides personnels automatiques grâce à leurs systèmes sensibles au contexte. Souvent, l'élément du contexte qui est utilisé dans ces applications est la position en deux dimensions (2 D). Toutefois, on peut envisager d'utiliser d'autres éléments de contexte.

Grâce aux capteurs d'un smartphone, on peut évaluer la position et l'orientation (sur les axes X, Y et Z). Ces données peuvent être utilisées pour transformer un smartphone en pointeur sur des objets intéressants dans l'espace tridimensionnel. L'expérience des utilisateurs devrait alors être améliorée. Cependant, les mesures fournies par les capteurs ne sont pas précises. C'est pourquoi nous proposons une fusion des capteurs pour diminuer cet inconvénient.

La fusion des capteurs peut être réalisée non seulement sur la base des capteurs internes du smartphone, mais aussi avec l'environnement l'extérieur. Dans le cas de géolocalisation à l'intérieur des bâtiments, l'approche « Wi-Fi Fingerprinting » est une des méthodes utilisées. C'est une méthode qui utilise des informations externes au smartphone. Même si les données provenant de l'intérieur et de l'extérieur du smartphone sont complètes, la qualité de leur fusion doit être étudiée pour assurer la faisabilité d'un usage du smartphone comme un outil de pointage à l'intérieur du bâtiment.

Cette étude propose une méthode pour estimer l'orientation et la position à l'aide de différents filtrages des données. Ces filtrages sont appelés respectivement « filtrage complémentaire » et « filtrage de Kalman ». Le filtrage complémentaire fait usage du gyroscope, du magnétomètre, et de l'accéléromètre qui appartiennent au système de navigation inertielle du smartphone. D'autre part, le filtrage de Kalman utilise l'accéléromètre et les données du "Wi-Fi Fingerprinting". Pour évaluer toutes ces estimations, l'affichage graphique et l'évaluation statistique sont présentées. Elles permettent de mesurer la qualité de filtrage dans le but de diminuer les erreurs.

Les résultats des analyses des performances des filtrages montrent que l'estimation d'orientation est relativement suffisante pour donner les angles acceptables. Mais, malheureusement, l'estimation de position a donné de mauvais résultats du fait de l'imprécision des capteurs et d'importants effets du « Wi-Fi Fingerprinting ». Les informations du « Wi-Fi Fingerprinting » donnent une position très imprécise en entrée du filtrage de Kalman, de même les données de l'accéléromètre sont très instables. Ces résultats montrent que

l'estimation de la position dans cette étude n'est pas suffisante pour des usages en situation réelle. Par contre, dans le test de pointage vers un objet en laboratoire, l'estimation d'orientation a donné une estimation relativement acceptable pour viser un objet lorsque la position du smartphone est fixée. En conclusion, l'estimation de la position et de l'orientation avec le filtrage complémentaire et le filtrage de Kalman ne se sont pas révélées pertinentes dans le cadre de cette étude. Toutefois, d'autres méthodes d'estimateur d'état pourraient être utilisées. De plus, d'autres mesures externes pourraient aider à réaliser une meilleure estimation de la position. Ces méthodes devraient toutefois consommer d'avantage d'énergie et ainsi risquer de réduire l'expérience de l'utilisateur.

Mot-clés: Systèmes sensible au contexte, géolocalisation intérieure, Wi-Fi Fingerprinting, Fusion des Capteurs

Contents

Thesis Recommendation Form iii

Abstrak v

Summary vii

Résumé ix

Contents xi

List of Figures xiii

List of Tables xv

1 Introduction 1
1.1 Motivational Background 1
1.2 Aim 2

2 Materials and Methods 3
2.1 Three dimensional position and orientation 3
2.2 Smartphone Inertial Navigation System sensors 4
2.2.1 Accelerometer 4
2.2.2 Gyroscope 4
2.2.3 Magnetometer 4
2.2.4 Sensor errors 5
2.3 Sensor Fusion 5
2.4 Radio Signal Strength Indication for Wi-Fi Fingerprinting . . . 5
2.4.1 Fingerprinting Offline Phase 6
2.4.2 Fingerprinting Online Phase 6
2.5 Weighted k-Nearest Neighbor 7
2.6 Kalman Filter 8
2.7 Complementary Filter 9

3 Analysis and Design 11
3.1 Environment 11
3.2 Workflow 12
3.2.1 Input 12
3.2.2 Prefiltering 13
3.2.3 Getting Rotation from *getRotationMatrix* Android API . 13

3.2.4 Complementary Filter 13
3.2.5 Wi-Fi Fingerprinting 14
3.2.6 Kalman Filter 14
3.3 Parameter Setup 15
3.3.1 Prefilter 15
3.3.2 Time Sampling 16
3.3.3 Complementary Filter 16
3.3.4 Calibration 16
3.3.5 Kalman Filter 17
3.3.6 Weighted K-Nearest Neighbor 17

4 Result and Discussion **19**
4.1 Wi-Fi Fingerprinting 19
4.1.1 Offline Phase 19
4.1.2 Online Phase 20
4.2 Filtering Result 21
4.2.1 Orientation Estimation by Complementary Filter 22
4.2.2 Position Estimation by Kalman Filter 26
4.3 Object Pointing by Smartphone 30
4.3.1 Object Pointing Scenario 1 30
4.3.2 Object Pointing Scenario 2 31
4.3.3 Summary 33

5 Conclusion **35**

A Wi-Fi RSSI Capture Sample **37**

B Complementary Filter Result **39**

C Kalman Filter Observation Data **43**

Bibliography **47**

List of Figures

Figure 2.1 Smartphone local coordinate system axis 3
Figure 2.2 fingerprinting phases offline and online phase 7
Figure 2.3 The relation of the two stages of Kalman Filter 9

Figure 3.1 The smartphones used in experiments: (a) Wiko Highway, (b) HTC One S, (c) Samsung Galaxy S4 11
Figure 3.2 Cropped map of experiment location 12
Figure 3.3 Proposed method flowchart 12

Figure 4.1 Wi-Fi Fingerprinting online phase result of Wiko Highway (a) and HTC One S (b) 21
Figure 4.2 The result of position estimation in X-axis (a), Y-axis (b), and Z-axis (c) by Kalman Filter of Wiko Highway, case: using only Linear Acceleration sensor data 27
Figure 4.3 The result of position estimation in X-axis (a), Y-axis (b), and Z-axis (c) Kalman Filter of HTC One S, case: using only Linear Acceleration sensor data 27
Figure 4.4 The result of position estimation in X-axis (a), Y-axis (b), and Z-axis (c) Kalman Filter of Wiko Highway, case: using only Linear Acceleration sensor data 28
Figure 4.5 The result of position estimation in X-axis (a), Y-axis (b), and Z-axis (c) Kalman Filter of HTC One S, case: using only Linear Acceleration sensor data 29
Figure 4.6 The objects for field evaluation: first scenario 30
Figure 4.7 Object for the field evaluation: second scenario 31
Figure 4.8 Orientation Estimation in pointing object (a) of Scenario 1 31
Figure 4.9 Orientation Estimation in pointing object (b) of Scenario 1 32
Figure 4.10 Orientation Estimation in pointing object of Scenario 2 . 33

Figure B.1 The result of Complementary Filter, case: No rotation (a) Wiko Highway (b) HTC One S (c) Samsung Galaxy S4 . . . 39
Figure B.2 The result of Complementary Filter, case: 90° Rotation over Z-axis (a) Wiko Highway (b) HTC One S (c) Samsung Galaxy S4 40
Figure B.3 The result of Complementary Filter, case: 90° Rotation over X-axis (a) Wiko Highway (b) HTC One S (c) Samsung Galaxy S4 40

Figure B.4 The result of Complementary Filter, case: 90° Rotation over Y-axis (a) Wiko Highway (b) HTC One S (c) Samsung Galaxy S4 41

Figure C.1 The linear acceleration observation of Kalman Filter of Wiko Highway in X-axis (a), Y-axis (b), and Z-axis (c), case: using only Linear Acceleration sensor data 43
Figure C.2 The linear acceleration observation of Kalman Filter of HTC One S in X-axis (a), Y-axis (b), and Z-axis (c), case: using only Linear Acceleration sensor data 44
Figure C.3 The linear acceleration observation of Kalman Filter of Wiko Highway in X-axis (a), Y-axis (b), and Z-axis (c), case: fusion of Linear Acceleration sensor data and Wi-Fi fingerprinting result 44
Figure C.4 The Wi-Fi positioning result observation of Kalman Filter of Wiko Highway in X-axis (a), Y-axis (b), and Z-axis (c), case: fusion of Linear Acceleration sensor data and Wi-Fi fingerprinting result 45
Figure C.5 The linear acceleration observation of Kalman Filter of HTC One S in X-axis (a), Y-axis (b), and Z-axis (c), case: fusion of Linear Acceleration sensor data and Wi-Fi fingerprinting result 45
Figure C.6 The Wi-Fi positioning result observation of Kalman Filter of HTC One S in X-axis (a), Y-axis (b), and Z-axis (c), case: fusion of Linear Acceleration sensor data and Wi-Fi fingerprinting result 46

List of Tables

Table 2.1 representation of collected RSSI $s_{i,j}$ of access point j of several positions p_i 6

Table 3.1 reference points of this study 14

Table 4.1 Offline Phase Averaged RSSI by Wiko Highway (sample) . 20
Table 4.2 Offline Phase Averaged RSSI by Samsung Galaxy S4 (sample) 20
Table 4.3 Offline Phase Averaged RSSI by HTC One S (sample) . . 21
Table 4.4 Evaluation of Orientation Estimation (Azimuth) of No-Rotation Case 22
Table 4.5 Evaluation of Orientation Estimation (Pitch,Roll) of No-Rotation Case 22
Table 4.6 Evaluation of Orientation Estimation (Azimuth) of Rotation over Z-axis Case 23
Table 4.7 Evaluation of Orientation Estimation (Pitch,Roll) of Rotation over Z-axis Case 23
Table 4.8 Evaluation of Orientation Estimation (Pitch) of Rotation over X-axis Case 24
Table 4.9 Evaluation of Orientation Estimation (Azimuth) of Rotation over X-axis Case 24
Table 4.10 Evaluation of Orientation Estimation (Roll) of Rotation over X-axis Case 24
Table 4.11 Evaluation of Orientation Estimation (Roll) of Rotation over Y-axis Case 25
Table 4.12 Evaluation of Orientation Estimation (Azimuth) of Rotation over Y-axis Case 25
Table 4.13 Evaluation of Orientation Estimation (Pitch) of Rotation over Y-axis Case 25
Table 4.14 Evaluation of Orientation Estimation in Pointing Object of Scenario 1 32
Table 4.15 Evaluation of Orientation Estimation in Pointing Object of Scenario 1 32

Table A.1 Captured RSSI by Wiko Highway S (sample) 37
Table A.2 Captured RSSI by Samsung Galaxy S4 (sample) 37
Table A.3 Captured RSSI by HTC One S (sample) 38

[This page is intentionally left blank]

Chapter 1

Introduction

1.1 Motivational Background

During cultural or tourism visits, a guide of the interesting objects is necessary to enhance the knowledge and the experience of the visitors. In these times, the mobile application using smartphones and tablets are possible to serve as an autonomous guide personally, in the case of context-aware system. The elements of the contexts of the users which mainly used in the visits are the positions, which will change in timely manner.

The guidance approach using the smartphone is composed in 3 dimensions, which are positions in X, Y, and Z, and the orientation in X, Y, and Z. Those dimensions are used in order to explore the possibility of smartphone of being pointer to interesting object, not for the position estimator only. Thus, the user experience should be possible to be increased, as they don't get vision-blocked (by always looking at the screen) or audio-blocked (by using an audio guidance headphones).

Unfortunately, determining the position and the orientation of the smartphone as the pointing guide, which is held by users, is probably not so accurate, especially in the indoor environment of a building without the aid of GPS [1]. The inertial navigation system [2] sensors included in a smartphone have many disadvantages. For example, accelerometer [3] to measure the displacement of the smartphone, but it tends to be highly noisy. Yet, the gyroscope [4], in measuring orientation, has some drawbacks in estimating the orientation since it has integration error called drifts. While the magnetometer [5] is easily disturbed by the magnetic field that produced by metal materials around the smartphone. Thus, an accurate estimation approach for the position and the orientation of the smartphone is important.

In the other hand, the approach in doing a combination or sensor fusion towards the smartphone sensors yields in a fine result [6–8] using some filters, namely Complementary Filter [7] and Kalman Filter [9]. However, these internal sensors are not very adequate to deal with precision of the trajectory. Hence, the external environment, such as WiFi, is used to improve the localization quality of the smartphone location and orientation [10, 11].

Some research results have considered the orientation estimation using 3D

Accelerometer and 3D magnetometer sensor fusion using Kalman Filter [9], combination of accelerometer, magnetometer, and gyroscope sensors in smartphone [7], and combination of heading (orientation in Z axis) plus the position tracking to do Indoor Positioning [8, 12, 13]. While the 3D position and orientation estimation by Kalman Filter have been provided by [8], it uses camera sensor, which in the purposed study it is not considered in this study because it blocks the vision. The more sophisticated heading and position estimation using Particle Filter and Dead Reckoning using Android Phone sensors and WiFi Fingerprinting has been conducted by [14], which positioning error reached up to 6 meters. Then, a newer approach of combining the WiFi Weighted Path Loss, Pedestrian Dead Reckoning using Smartphone sensors, and Landmarks [11] also give a good positioning error result about 1 meter. Without WiFi aid, the native sensors of smartphone [8] provided small error about 0.3% in heading measurement and 0.8 meters in position estimation. However, there isn't much specific measurement and evaluation toward 3D position and 3D orientation estimation to aid the object-pointing which mostly will be considered in this study.

Then, the purpose of this study is to explore the possibility to gain the 3D position and orientation estimation by the smartphone and WiFi fingerprinting. Thus, the smartphone can be a decent yet affordable tool to be a guide in a visit, yet its possibility to be an aid for the visually impaired also.

1.2 Aim

The aim of this project is to study the possibility of data fusion of smartphone sensors and Wi-Fi fingerprinting to make a smartphone as a precise pointing object.

Chapter 2

Materials and Methods

In this section, the materials and method related to this study will be explained. The related material studied are smartphone 3D orientation and position; Inertial Navigation System (INS) sensor aspects related to smartphone, which are accelerometer, gyroscope, and magnetometer; and Wi-Fi Radio Signal Strength Indication (RSSI). The methods that will be explained are the Kalman Filter; Complementary Filter; and Wi-Fi fingerprinting, where the deterministic positioning algorithm, the weighted k-Nearest Neighbor, was applied.

2.1 Three dimensional position and orientation

The three dimensional position and orientation in this study is represented in 3-axis coordinates X, Y, Z and their representation in the smartphone local frame. This representation of the position and orientation is important because the sensors only know their position and orientation locally. In further application, this local reference can be transformed into global reference. This representation is depicted in Figure 2.1.

The orientation angles in 3D are called roll, pitch, and yaw (or azimuth, in several references, for example [15]) in X, Y, Z axes respectively. Even though they are measured locally by the smartphone, if the help of digital compass (will be explained later) is being used, the direction towards north global reference can be approximated.

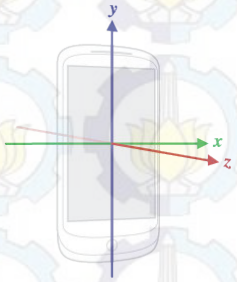

Figure 2.1: Smartphone local coordinate system axis

2.2 Smartphone Inertial Navigation System sensors

The smartphone INS sensors which will be studied in this project are the accelerometer, gyroscope, and the magnetometer. The accelerometer measures the acceleration of the smartphone movement, the gyroscope measures the rotation of the orientation of the smartphone, and the magnetometer measures the magnetic field around the smartphone. The API derived sensors, gravity and linear acceleration, will be explained also in the Accelerometer subsection.

2.2.1 Accelerometer

The accelerometer measures the *proper acceleration* of the device. Thus, it is a little bit different to the acceleration in space. This acceleration is related to the weight experienced by a test mass which placed in the frame of reference of the accelerometer device. In general, the acceleration is measured by the pressure of a mass on something when a force occurs [1].

A resting device's accelerometer relative to the earth's surface will experience acceleration of approximately 1G upwards. Because any point on the Earth's surface is accelerating upwards relative to the local inertial frame (the frame of a freely falling object near the surface).

Thus, in this case, acceleration of the accelerometer can be composed from two different accelerations. The first part is the gravity acceleration and the second part is the linear acceleration. The gravity acceleration is the acceleration that happened because of the gravity, while the linear acceleration is the acceleration in the device that happens excluding gravity. The simple representation of these two components as represented in (2.1). These two components can be derived from the Android API if available in the device [16].

$$linear\ acceleration = acceleration_{accelerometer} - gravity \tag{2.1}$$

2.2.2 Gyroscope

A gyroscope is used to measure orientation of a device by the principle of conservation of angular momentum. In case of smartphone, MEMS (Micro Electro-Mechanical System) type of gyroscope is applied. This type of gyroscope has vibrating elements to sense the Coriolis effect. In this type of gyroscope, single mass tends to vibrate along a drive axis. When the gyroscope is rotated, a secondary vibration happened along the perpendicular sense axis due to the Coriolis force. Thus, by measuring the secondary rotation, the angular velocity can be calculated. Unlike the accelerometer and the magnetometer, the Gyroscope measures angular velocity locally [1].

2.2.3 Magnetometer

Magnetometer measures the strength of magnetic field in the surrounding environment. The magnetometer applied in this case are the vector magnetometer

instead of the scalar magnetometer. It has the capability to measure the component of magnetic field in certain direction regarding to the local reference of the device [1]. This is important to this study because the magnetometer should be enabled as digital compass.

2.2.4 Sensor errors

The sensors provided in the smartphone are not all perfect. Because of internal and external disturbances, they tend to have errors in the measurement process [1].

The accelerometer, due to its nature to be noisy, has a terrible error to measure the position directly. This error is derived from the double integration from the acceleration. It is possible to estimate the bias by subtracting the long term average of the accelerometer's output from the current measurement.

Then, the gyrocope produces the drift error after the device is rotated, aside of the integration error from the angular velocity to the angular orientation. This error's magnitude is related to the rate and duration of the rotation. This error can be horrible in addition to the initial integration error.

The magnetometer's error is related to the disturbance from metallic material around the sensor. Beside that, if the sensor is rotated while acquiring the measurement, additional error is generated.

2.3 Sensor Fusion

Sensor fusion is a method to combine data which came from different sensors to yield "better" information in spite of individual sensor data. This "better" can be related into several meanings, which are more accurate, more precise, more complete, or more dependable [1, 17]. This sensor fusion can be worked with several filtering methods, such as Complementary Filter or Kalman Filter, which will be discussed later. This fusion involves two or more different sensors toward the filter. So, that the measurements will acquire better performance.

2.4 Radio Signal Strength Indication for Wi-Fi Fingerprinting

Radio Signal Strength Indication (RSSI) measurement in several location can be different each other. Thus, it can be used as fingerprint. A single vector of RSSI values are obtained by a measurement process in a location which will capture the signal strength by nearby Wi-Fi access points. The RSSI in noise free environment can be modeled using (2.2) [10].

$$RSSI = P - R - 10\alpha log_{10} d \tag{2.2}$$

The variables of (2.2) is described as follows. The $RSSI$ is the value of RSSI in dBm (decibel-miliwatt). P is the power of transmission, α is the

Table 2.1: representation of collected RSSI $s_{i,j}$ of access point j of several positions p_i

	Captured RSSI at several positions					
p_1	$s_{1,1}$	$s_{1,2}$	$s_{1,3}$	$s_{1,4}$	...	$s_{1,n}$
p_2	$s_{2,1}$	$s_{2,2}$	$s_{2,3}$	$s_{2,4}$	...	$s_{2,n}$
p_3	$s_{3,1}$	$s_{3,2}$	$s_{3,3}$	$s_{3,4}$	...	$s_{3,n}$
p_4	$s_{4,1}$	$s_{4,2}$	$s_{4,3}$	$s_{4,4}$	...	$s_{4,n}$
p_5	$s_{5,1}$	$s_{5,2}$	$s_{5,3}$	$s_{5,4}$	...	$s_{5,n}$
...			...			
p_m	$s_{m,1}$	$s_{m,2}$	$s_{m,3}$	$s_{m,4}$	...	$s_{m,n}$

path loss exponent which linearly falls, R is a constant which influenced by the condition of the environment, and d is the distance of the measuring point to the access point. The device used to capture the measurement has to have the capability to capture the Wi-Fi signal, in this case, it can be smartphone, personal computer (PC), or notebooks.

Sometimes, single sample of RSSI measurement is not sufficient to characterize a fingerprint. It is because the environment or the device capturing quality can heavily affect the measurement. Thus, it is necessary to average several measurement samples to get a fingerprint. The captured RSSI measurements from several access points is the collection which characterize the single fingerprint of location.

The fingerprinting is based on two stages. They are the offline phase, the collection phase, and the online phase, the position calculation phase.

2.4.1 Fingerprinting Offline Phase

In this phase, a training set of offline fingerprints will be gathered using the capturing device. The RSSI $\mathbf{s}_i, j$ of access point j are collected within the position p_i of the capturing device. Considering the successfully captured RSSI of n distinct access points in several m positions, the representation of the measurement is depicted in Table 2.1.

2.4.2 Fingerprinting Online Phase

In this phase, a fingerprint of a location will be captured from the device. The RSSI $\mathbf{s}_j^*$ of several access points j within the position p^* will be compared to existing RSSI collection database which collected during the offline phase. This comparison method results estimation of position of the device according to the RSSI collection. That comparison method can be also called positioning. An illustration of online and offline phase is depicted in Figure 2.2.

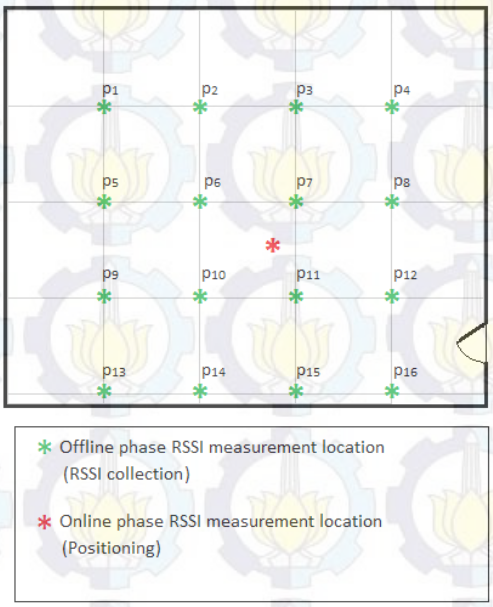

Figure 2.2: fingerprinting phases offline and online phase

2.5 Weighted k-Nearest Neighbor

This positioning is classified as deterministic algorithm to compute the possible position from captured RSSI from a location [18]. This algorithm is based on distance between the captured RSSI at the capturing location and the provided RSSI in offline database from the same access point. However, if there is a RSSI from an access point of captured location which does not exist in the database or vice versa, that RSSI will be omitted from the calculation. The signal distance L_q between a single position $\mathbf{s}$ in the offline database and at the captured location $\mathbf{s}^*$, where n access points are identified, is described in (2.3).

$$L_q = \left(\sum_{j=1}^{n} |s_j^* - s_j|^q \right)^{\frac{1}{q}} \tag{2.3}$$

The equation above, which based on Minkowski distance, has parameter $q(q \geq 1)$ to determine the order of distance. The most frequently used q values are 1 and 2, which called Manhattan (City-block) and Euclidean distance.

The nearest neighbor algorithm acquires the nearest point to the captured location by the distance defined in (2.3) (the most minimum distance). Meanwhile, the k-nearest neighbor algorithm takes k nearest neighbors from the distance, which then the position is calculated by averaging the k positions.

Similar to k-nearest neighbor, the Weighted k-Nearest Neighbor uses the averaging method to determine a position. But, in addition the scheme of weighting is introduced. This weighting scheme is based on the inverse distance of each nearest neighbor, as expressed in (2.4), where $i \in 1, 2, ..., k$. The

position p^* where the RSSI vector are captured is defined in (2.5).

$$w_i = \frac{1}{d_i} \tag{2.4}$$

$$p^* = \frac{\sum_{i=1}^{k} w_i p_i}{\sum_{i=1}^{k} w_i} \tag{2.5}$$

2.6 Kalman Filter

Kalman Filters is a type of widely used Bayesian filter because of its computational efficiency [11]. The Kalman Filter by R.E. Kalman [19], which this research will be benefit from, estimates a state $x \in \Re^n$ of a discrete-time controlled process which conserved by linear stochastic difference equation (2.6) and measurement $z \in \Re^m$ (2.7). The state has n dimensions of the process to be estimated and the measurements has m dimensions of measurements to be observed.

$$x_k = Ax_{k-1} + Bu_{k-1} + w_{k-1} \tag{2.6}$$

$$z_k = Hx_k + v_k \tag{2.7}$$

State estimation at time step k (2.6) is described as follows. It involves the matrix A related to the previous time step state x_{k-1}. The dimension of state transition model matrix A is $n \times n$ identity matrix. It also involves control input $u \in \Re^p$ (if available in the process) of previous time step and input model matrix B which dimension in $n \times l$ regarding the case of the input (dimension $l \times 1$) to the process. Then, random variable w is considered as process noise.

In the other hand, the measurement at time step k (2.7) is described using different variable and matrices. The measurement matrice H maps the state x_k into dimension of measurement. Matrice H has $n \times m$ dimension. The variable v_k is the measurement noise.

The random variable w_k and v_k assumed to have no correlation each other, white noise, and normal probability distributions, expressed in (2.8) and (2.9).

$$p(w) \sim N(0, Q) \tag{2.8}$$

$$p(v) \sim N(0, R) \tag{2.9}$$

Practically, the process noise covariance Q and measurement noise covariance R matrices of $n \times n$ and $m \times m$ respectively can be considered constant. However, they have the probability to change over time step or measurement.

The Kalman Filter's procedure divided into two stages: time update and measurement update. The time update stage is responsible for the predicting the current state and error covariance to acquire the *a priori* estimation for the next time step. The measurement update stage is responsible to give feedback to the estimation, for example to take in the new measurement to the *a priori* estiation to acquire the improved *a posteriori* estimate. Those two stages, time update and measurement update, are connected each other

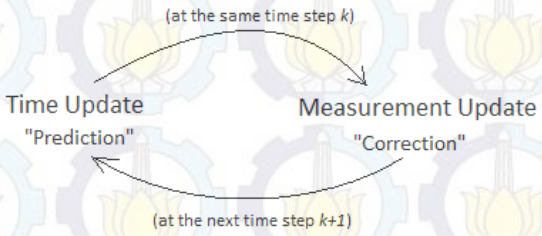

Figure 2.3: The relation of the two stages of Kalman Filter

and called *predictor-corrector* algorithm. The graphical representation of this relationship is depicted in Figure 2.3.

$$\hat{x}_k^- = A\hat{x}_{k-1}^- + Bu_k + Q \tag{2.10}$$

$$P_k^- = AP_{k-1}^- A^T + R \tag{2.11}$$

The time update stage is represented by (2.10) and (2.11). The matrices A and B are from the previous (2.6), while the matrix from (2.8). The time update for the state estimation (2.10) predicts the state x at the time step k by the estimation (using $\hat{}$) and before the measurement update (using minus sign "$-$" superscript). Using the same before measurement update term, the time update for the error covariance (2.11) predicts P before the measurement update (using minus sign "$-$" superscript).

$$K_k = P_k^- H^T (HP_k^- H^T + R)^{-1} \tag{2.12}$$

$$\hat{x}_k = \hat{x}_k^- + K_k(z_k - H\hat{x}_k^-) \tag{2.13}$$

$$P_k = (I - K_k H)P_k^- \tag{2.14}$$

The measurement update stage is represented by (2.12), (2.13), and (2.14). The matrix H in those three equations came from (2.7). The first step in measurement update is to calculate the Kalman Gain K_k (2.12). The matrix R is derived from (2.9). The next step is to acquire "corrected" estimation state $\hat{x}_k$ by the residual obtained from the subtraction of measurement z_k and the predicted observation $H\hat{x}_k^-$ times the gain K_k (2.13). Then, *a posteriori* error covariance estimation is obtained from (2.14), considering I is identity matrix of dimension of $n \times n$.

2.7 Complementary Filter

The complementary filter is an alternative from the Kalman Filter to combine two different measurements. The application of this filter is toward the angle estimation [7, 20]. This filter mainly consists of the low pass filter and high pass filter. Then, there are two important components also namely sample period and time constant.

The low pass filter and high pass filter in the complementary filter has opposite goals. The low pass filter has goal to pass out the long term change

to the result, avoiding short term but high fluctuation. This characteristic fits a noisy measurements, such as accelerometer. While the high pass filter has to avoid the slight but consistent change in the measurement. Thus, this characteristic has possibility to cancel out drift. This nature suits the drifting measurement, for example gyroscope.

Considering there are two measurements accelerometer *acc* and gyroscope *gyro*. The fusion using complementary filter can be written as (2.15), where the desired measurement θ_k is angular position at time step k.

$$\hat{\theta}_k = \alpha(\hat{\theta}_{k-1} + \omega_{k_{gyro}}\delta t) + (1-\alpha)(\theta_{k_{acc}}) \tag{2.15}$$

The sample period δt and time constant τ affects the filter coefficient α in (2.15), which relationship is described in (2.16). The filter coefficient drives the influence of high pass filter and low pass filter to each measurement. The sample period is the time interval between each execution of the filter action. Then, the time constant is the relative duration of signal it will act on.

$$\alpha = \frac{\tau}{\tau + \delta t} \tag{2.16}$$

Chapter 3

Analysis and Design

In this chapter, the implementation of the proposed study will be discussed. The purpose of this chapter is to give explanation about the environment, the workflow, and the parameter setup.

3.1 Environment

This study utilized several tools and executed in several conditions. Three smartphones will be utilized to analyze their sensors' performance in this study. Those three smartphone are Wiko Highway, HTC One S, and Samsung Galaxy S4, which are presented in Figure 3.1. The map of the whole floor is depicted in Figure 3.2, where the location of the experiment is orange-colored. The room has size of 7 m x 6 m. This environment is also equipped by a nearest Wi-Fi access points is also included in the map which is indiced by blue rectangle.

All part of this study is implemented in Java environment. The programming is conducted in Android Studio. All the smartphones have different version of Android. To share the data estimated by the smartphone, a TCP/IP connection to the PC is made.

The location of experiment is heavily barricaded by laboratory furniture, yet many electronic devices inside. Thus, it can drive to a highly noisy mag-

(a) (b) (c)

Figure 3.1: The smartphones used in experiments: (a) Wiko Highway, (b) HTC One S, (c) Samsung Galaxy S4

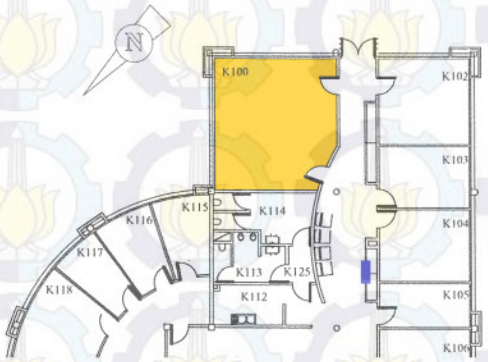

Figure 3.2: Cropped map of experiment location

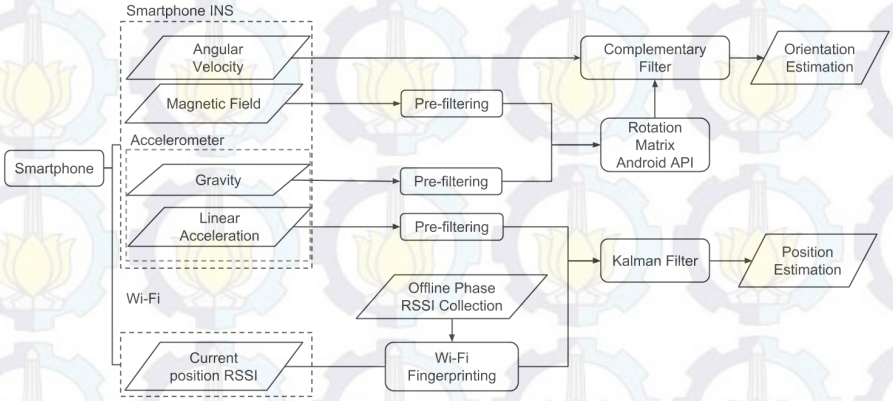

Figure 3.3: Proposed method flowchart

netometer data and weak Wi-Fi signal strength. However, this condition is feasible in the real world application, since the decoration of the room is still unknown and there are numerous possible indoor arrangement.

3.2 Workflow

The workflow of this study is represented in Figure 3.3. All the inputs are captured individually by sensors of single smartphone. The expected output is the estimation of orientation $\hat{\theta}_{x,y,z}$ and the estimation of position $\hat{p}_{x,y,z}$, which were already corrected and experiencing the sensor fusion by the Complementary and the Kalman Filter, respectively. Those steps and data will be explained below.

3.2.1 Input

The input data used in this study is represented by the five data received by smartphone. They are the angular velocity $\omega_{x,y,z}$ in $rad/s$from the gyroscope, the magnetic field strength $mag_{x,y,z}$ in μT from the magnetometer, the gravity force $g_{x,y,z}$ and the linear acceleration $a_{x,y,z}$ from the accelerometer, both in

m/s^2 and finally the vector of RSSI reading of available access points $\boldsymbol{s}$ in dB.

3.2.2 Prefiltering

The prefiltering will be applied for the noisy sensors, which are accelerometer and magnetometer. This prefiltering is used to smoothen the observation data, which then considered as input for the next method for each measurement. The prefilter consisted of the averaging filter then the median filter. Both filtering method employed a frame of N moving windows towards previously recorded set of data $\{o_{i-N}, o_{i-(N-1)}..., o_{i-1}, o_i\}$ to gather filtered observation o'_i, where i should be not less than N. The averaging filter for averaged observation data described in (3.1). After that, the median filter gets the desired observation o'_i from sorted $\{o_{i-N}, o_{i-(N-1)}..., o_{i-1}, o_i\}$, then getting its middle point (i) value.

$$a = i - N; b = i; o'_i = \frac{\sum_{j=a}^{b} o_j}{N} \tag{3.1}$$

The sequence of $\{o_{i-N}, o_{i-(N-1)}..., o_{i-1}, o_i\}$ is more preferred than $\{o_{i-\frac{N}{2}}, ..., o_i, ..., o_{i+\frac{N}{2}}\}$ because the after i-th datum, it has to wait for more $\frac{N}{2}$ data to arrive at the moving window. This might affect the filtering performance to provide the not up-to-date data. Thus, the estimation can be long enough to have a real-time data. However, this scheme has some drawbacks to be discussed in the parameter setup section.

3.2.3 Getting Rotation from *getRotationMatrix* Android API

The rotation angle by the geomagnetic field (from the magnetometer) and gravity (from the gravity sensor, derived from the accelerometer) can be derived from the Android API [15] by the *getRotationMatrix(...)* public method. The method result two matrices: the Rotation matrix and the Inclination matrix. However, the Rotation Matrix only that used for the input of Complementary Filter.

3.2.4 Complementary Filter

As discussed in previous chapter, the complementary filter takes input from the gyroscope measurement and prefiltered digital compass measurement from the rotation matrix API. By considering the three orientation, representing roll, pitch and azimuth (x,y, and z axis), the equation (2.15) is modified as described in (3.2).

$$\begin{bmatrix} \hat{\theta}_{x,k} \\ \hat{\theta}_{y,k} \\ \hat{\theta}_{z,k} \end{bmatrix} = \alpha \begin{bmatrix} \hat{\theta}_{x,k-1} + (\omega_{x,k} * \delta t) \\ \hat{\theta}_{y,k-1} + (\omega_{y,k} * \delta t) \\ \hat{\theta}_{z,k-1} + (\omega_{z,k} * \delta t) \end{bmatrix} + (1 - \alpha) \begin{bmatrix} \theta_{x,k} \\ \theta_{y,k} \\ \theta_{z,k} \end{bmatrix} \tag{3.2}$$

Table 3.1: reference points of this study

Position	x	y	z
p_A	0.5	0.5	1.25
p_B	3	0.5	1.25
p_C	5.5	0.5	1.25
p_D	0.5	2	1.25
p_E	3	2	1.25
p_F	5.5	2	1.25
p_G	0.5	3.5	1.25
p_H	3	3.5	1.25
p_I	5.5	3.5	1.25
p_J	0.5	5	1.25
p_K	3	5	1.25
p_L	5.5	5	1.25

The $\left[\hat{\theta}_{x,k}\ \hat{\theta}_{y,k}\ \hat{\theta}_{z,k}\right]^T$ are the estimated orientation in three axis for the outputs. While for the inputs are $\left[\omega_{x,k}\ \omega_{y,k}\ \omega_{z,k}\right]^T$ are the angular velocities in 3-axis from gyroscope and $\left[\theta_{x,k}\ \theta_{y,k}\ \theta_{z,k}\right]^T$ are the orientations from digital compass.

The parameter setup for α will be discussed later. It related to the time sample of the estimation, which also need to be discussed before. The time constant parameter of alpha regarding (2.16) will be determined also through the discussion.

3.2.5 Wi-Fi Fingerprinting

The fingerprinting locations of offline phase of the experiment room are spread into 14 reference points. These points vary in the position axis of x and y, but not in z axis, within natural human reach in the room (it is not possible to take z position of 4 m by hand, for example). Those three smartphones are used to capture the RSSI signal of these 12 points. Those points are detailed in Table 3.1.

The RSSI capturing process in the offline phase is triggered each 0.75 s and takes place 30 times. Thus, the smartphone must be held for around 22.5 seconds to get full measurements. Then, these 30 measurements are averaged within 5 measurements before inserted into the offline database for positioning. This is performed to avoid strict difference from each signal, which then resulted in more flexible weighing process.

3.2.6 Kalman Filter

The equation of system model of the Kalman Filter (3.3) is a linear state space and its transition matrix presented in (3.4), where the states are the position, velocity, and acceleration in 3 axis of local phone reference, respectively. There is no input for the Kalman Filter. The observation (3.5) will be decided into two different values by different experiments. The first value is provided by

accelerometer only, thus the observation variables will be 3 (3.6). Then, the second value is 6 (3.7), where Wi-Fi can provide positioning variables.

$$\hat{\mathbf{x}}_k = A\hat{\mathbf{x}}_{k-1} + Q \tag{3.3}$$

where

$$A = \begin{bmatrix} 1 & 0 & 0 & \delta t & 0 & 0 & \frac{\delta t^2}{2} & 0 & 0 \\ 0 & 1 & 0 & 0 & \delta t & 0 & 0 & \frac{\delta t^2}{2} & 0 \\ 0 & 0 & 1 & 0 & 0 & \delta t & 0 & 0 & \frac{\delta t^2}{2} \\ 0 & 0 & 0 & 1 & 0 & 0 & \delta t & 0 & 0 \\ 0 & 0 & 0 & 0 & 1 & 0 & 0 & \delta t & 0 \\ 0 & 0 & 0 & 0 & 0 & 1 & 0 & 0 & \delta t \\ 0 & 0 & 0 & 0 & 0 & 0 & 1 & 0 & 0 \\ 0 & 0 & 0 & 0 & 0 & 0 & 0 & 1 & 0 \\ 0 & 0 & 0 & 0 & 0 & 0 & 0 & 0 & 1 \end{bmatrix}, \hat{\mathbf{x}}_k = \begin{bmatrix} x \\ y \\ z \\ \dot{x} \\ \dot{y} \\ \dot{z} \\ \ddot{x} \\ \ddot{y} \\ \ddot{z} \end{bmatrix} \tag{3.4}$$

$$\mathbf{z}_k = H\hat{\mathbf{x}}_k + R \tag{3.5}$$

where

$$H = \begin{bmatrix} 0 & 0 & 0 & 0 & 0 & 0 & 1 & 0 & 0 \\ 0 & 0 & 0 & 0 & 0 & 0 & 0 & 1 & 0 \\ 0 & 0 & 0 & 0 & 0 & 0 & 0 & 0 & 1 \end{bmatrix}, \mathbf{z}_k = \begin{bmatrix} \ddot{x} \\ \ddot{y} \\ \ddot{z} \end{bmatrix} \tag{3.6}$$

or

$$H = \begin{bmatrix} 1 & 0 & 0 & 0 & 0 & 0 & 0 & 0 & 0 \\ 0 & 1 & 0 & 0 & 0 & 0 & 0 & 0 & 0 \\ 0 & 0 & 1 & 0 & 0 & 0 & 0 & 0 & 0 \\ 0 & 0 & 0 & 0 & 0 & 0 & 1 & 0 & 0 \\ 0 & 0 & 0 & 0 & 0 & 0 & 0 & 1 & 0 \\ 0 & 0 & 0 & 0 & 0 & 0 & 0 & 0 & 1 \end{bmatrix}, \mathbf{z}_k = \begin{bmatrix} x \\ y \\ z \\ \ddot{x} \\ \ddot{y} \\ \ddot{z} \end{bmatrix} \tag{3.7}$$

The parameters in the equation, which are covariance of matrices Q and R, will be discussed later. These parameters are necessary to define the noise error that should be considered in the practice.

3.3 Parameter Setup

In this section, the necessary parameters in this study will be discussed. They are the parameters regarding the prefiltering (averaging and median window length), the time sample of estimation for both Complementary Filter and Kalman Filter, the time constant for Complementary Filter, the neccessity for calibration of the sensor, the noise error covariance of Kalman Filter and the k Weighted k-NN.

3.3.1 Prefilter

This prefiltering, which consisted of averaging filter and median filter, has a moving window element to reduce the noisy measurements. The important parameter of this filter is the window length N, which used for both averaging

filter and median filter. The bigger the N, the prefiltering can give smoother measurements to be input of state estimation. However, this big N value has drawback to have a very old data affecting the current measurement.

Thus, considering the fastest time delay of the sensor that can be captured, which is 10 ms, and the time sampling δt (which will be discussed later), the window length N is defined to 10. This leaves up the latest considered data is at 100 ms before, in the best assumption if the sensor always change its measurement in that time frame.

3.3.2 Time Sampling

The time sampling for the estimation (Kalman Filter, Complementary Filter) is very important. The definition of the time sampling must be slower than the observer, which are the sensors. The sensors has capability to provide 10 ms short of update (if there's any change in the measurement, for example: the smartphone moves, the smartphone rotates). Thus, the time sample for the estimation must be slower than the observation change time. Finally, the defined time sample is 20 ms for this study.

Regarding the prefiltering case, the window length N affects the performance by taking this defined time sampling value into account. The estimation is only going to be affected by the five (5) previous sensor changes in 100 ms.

Although the time sampling is fast enough to handle the sensor change, it cannot match with the slow Wi-Fi RSSI capture. In the offline phase, the Wi-Fi RSSI indicates its strength change after 3 seconds interval at a location. Thus, this time difference between sensor change and the Wi-Fi strength change can be problematic. However, the time sample cannot be set to achieve the slow Wi-Fi RSSI capture time, since it can heavily influence the state estimation based on the sensor. Hence, the time sample is left to be 20 ms.

3.3.3 Complementary Filter

In the Complementary Filter, the parameter which heavily affects which the passing of High Pass Filter and Low Pass Filter is α, which is produced by the time constant and time sample as described in (2.16). As the time sample has been defined, the only task left is to define the time constant. After several experiments, using the relativity of the smoothness, the value of 750 ms is used.

3.3.4 Calibration

Calibration is a process to correcting the observations to base level. In this study, the calibrated sensor is the linear acceleration. Initially this is used to avoid the high double integration error caused by the wrong estimation in the beginning. The calibration process starts from the data collecting until N data has been collected. The next process is average those N data. The result of this average will then used as subtraction for the next measurement.

3.3.5 Kalman Filter

As mentioned before, the error noise estimation matrix' covariance Q and measurement matrix' covariance R are important to minimize the noise which happened both in the estimation and the measurements observation. Even though so, to find good approximation of these parameters is very exhaustive, because it could be ranged from the smallest value near 0 until the biggest possible.

To solve this approximation problem, we have conducted a parameter research between 10^{-6} until 10^{5}, by the step of multiplication by 10. And finally, we have decided the value of Q of 1 and R of 10. These values are based on the noises removal quality by Kalman Filter.

3.3.6 Weighted K-Nearest Neighbor

The weighted K-Nearest Neighbor has two considered parameters, which are neares neighbor k and the type of distance. The number of nearest neighbor k, as studied by [18], is defined to be 3. And the distance uses the Euclidean distance (Minkowski distance where $q = 2$).

[This page is intentionally left blank]

Chapter 4

Result and Discussion

In this chapter, the results from the proposed study will be presented.The sample of captured Wi-Fi RSSI by smartphone by tabular representation, before the evaluation scenario results in the previous chapter. Then, the previously described filter results scenario will be presented. Thus, the final scenario results are going to be shown in the last part.

4.1 Wi-Fi Fingerprinting

In this section, the result of Wi-Fi fingerprinting will be presented. The first part will explain about the result of the offline phase, which is the RSSI collecting into database. The second part will describe about the result of the Wi-Fi positioning using weighted k-Nearest Neighbor.

4.1.1 Offline Phase

The offline phase of Wi-Fi fingerprinting is performed by the three smartphones in the locations as specified in Table 3.1. The captured RSSI values below -90 are ignored. This is because the weak signal might disturb the positioning algorithm. The zero value (0) in the table indicated means the signal from that single access point is ignored (below -90) or not found.

The captured RSSI signal sample of 7 access points of each position from the three smartphones are presented as follows. By Wiko Highway S, the captured RSSI, which were originally from 48 access points, are presented in Table A.1. Samsung Galaxy S4 successfully captured RSSI from 50 access points, which samples are presented in Table A.2. And finally, HTC One S captured RSSI from 29 access points, which samples are presented in Table A.3.

Then, the sample of result of Wi-Fi Fingerprinting Offline phase, which is averaged RSSI measurements of each location, are presented as follows. The offline phase result of Wiko Highway, Samsung Galaxy S4, and HTC One S are presented in Table 4.1, Table 4.2, and Table 4.3 respectively.

Then, the characteristics of this offline phase of each smartphone is described as follows. From the results presented by the tables, it can be found

Table 4.1: Offline Phase Averaged RSSI by Wiko Highway (sample)

Position (x,y,z)	Access Points						
	AP_1	AP_2	AP_3	AP_4	AP_5	AP_6	AP_7
p_A(0.5,0.5,1.25)	-88	-89	-65	-62	-69	-70	-62
p_B(3,0.5,1.25)	0	-89	-67	-67	-68	-67	-65
p_C(5.5,0.5,1.25)	0	-89	-70	-64	-70	-70	-64
p_D(0.5,2,1.25)	0	-89	-68	-67	-67	-67	-67
p_E(3,2,1.25)	0	0	-71	-65	-77	-71	-64
p_F(3,2,1.25)	0	0	-69	-65	-70	-74	-64
p_G(0.5,3.5,1.25)	0	0	-68	-71	-62	-62	-71
p_H(3,3.5,1.25)	0	-89	-74	-68	-65	-75	-68
p_I(3,3.5,1.25)	0	-89	-64	-69	-64	-73	-70
p_J(0.5,5,1.25)	0	0	-73	-63	-62	-62	-64
p_K(3,5,1.25)	0	0	-67	-73	-67	-70	-72
p_L(3,5,1.25)	-86	0	-62	-66	-62	-67	-66

Table 4.2: Offline Phase Averaged RSSI by Samsung Galaxy S4 (sample)

Position (x,y,z)	Access Points						
	AP_1	AP_2	AP_3	AP_4	AP_5	AP_6	AP_7
p_A(0.5,0.5,1.25)	-77.8	-69.2	-75	-73	-78	-78.2	-67.6
p_B(3,0.5,1.25)	-71	-66.2	-71.6	-71	-71	-72	-67.4
p_C(5.5,0.5,1.25)	-70.2	-61.2	-70.6	-71.2	-73	-70.6	-59.6
p_D(0.5,2,1.25)	-68	-66	-66.6	-67.4	-68	-78.2	-65.4
p_E(3,2,1.25)	-72.6	-64.8	-71.6	-72.6	-72.6	-73	-64.4
p_F(5.5,2,1.25)	-72.8	-64	-72.4	-72.2	-73	-72.8	-64.8
p_G(0.5,3.5,1.25)	-74.4	-72.4	-72.8	-72.8	-74.8	-77.8	-72.2
p_H(3,3.5,1.25)	-68.2	-66.6	-67.2	-68.4	-68.6	-67.2	-67.4
p_I(5.5,3.5,1.25)	-63.6	-74.4	-63.4	-63.8	-63.6	-64	-70.8
p_J(0.5,5,1.25)	-63.4	-70	-63	-63.4	-65.2	-65.8	-70.4
p_K(3,5,1.25)	-71.4	-72.4	-70.8	-70.2	-70.2	-69.8	-67.2
p_L(5.5,5.1.25)	-67.2	-73.6	-66.2	-66.2	-66	-67	-73

that the RSSI capture by the Wiko Highway S has higher tendency to be ignored or not found. This can be inferred by the more zero values than the others. Also, the Wiko Highway has no averaged results of decimal points. This can mean two possibilities. The first, the Wi-Fi signal sensor of Wiko Highway is less insensitive than the others. Or the second, the Wi-Fi signal sensor of Wiko Highway has slower Wi-Fi refreshing frequency than the others.

4.1.2 Online Phase

The online phase of the Wi-Fi fingerprinting was performed by two smartphones: Wiko Highway and HTC One S. Samsung Galaxy S4 cannot be used because it was not available at the moment. The two smartphone performed the online phase at the exact same position. But, they produced different results. The online phase was performed around 20 seconds. The graphical representation of their performances were depicted in Figure 4.1.

By the result of Online Phase, it could be inferred that the Wi-Fi finger-

Table 4.3: Offline Phase Averaged RSSI by HTC One S (sample)

Position (x,y,z)	Access Points						
	AP_1	AP_2	AP_3	AP_4	AP_5	AP_6	AP_7
p_A(0.5,0.5,1.25)	-77.8	-69.2	-75	-73	-78	-78.2	-67.6
p_B(3,0.5,1.25)	-71	-66.2	-71.6	-71	-71	-72	-67.4
p_C(5.5,0.5,1.25)	-70.2	-61.2	-70.6	-71.2	-73	-70.6	-59.6
p_D(0.5,2,1.25)	-68	-66	-66.6	-67.4	-68	-78.2	-65.4
p_E(3,2,1.25)	-72.6	-64.8	-71.6	-72.6	-72.6	-73	-64.4
p_F(5.5,2,1.25)	-72.8	-64	-72.4	-72.2	-73	-72.8	-64.8
p_G(0.5,3.5,1.25)	-74.4	-72.4	-72.8	-72.8	-74.8	-77.8	-72.2
p_H(3,3.5,1.25)	-68.2	-66.6	-67.2	-68.4	-68.6	-67.2	-67.4
p_I(5.5,3.5,1.25)	-63.6	-74.4	-63.4	-63.8	-63.6	-64	-70.8
p_J(0.5,5,1.25)	-63.4	-70	-63	-63.4	-65.2	-65.8	-70.4
p_K(3.5,1.25)	-71.4	-72.4	-70.8	-70.2	-70.2	-69.8	-67.2
p_L(5.5,1.25)	-67.2	-73.6	-66.2	-66.2	-66	-67	-73

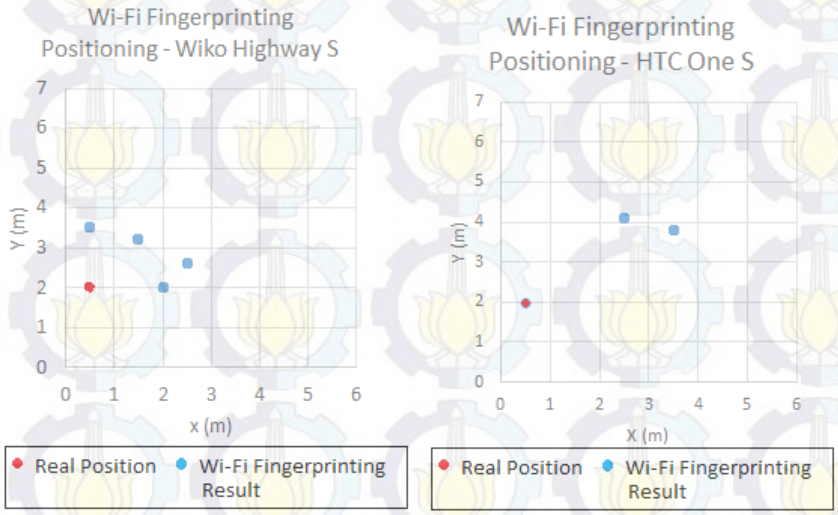

(a) (b)

Figure 4.1: Wi-Fi Fingerprinting online phase result of Wiko Highway (a) and HTC One S (b)

printing gave errors about 1,5-3 meters from the actual position. Thus, an improvement toward the position observation should be performed. Those improvement could be adding the reference points or using other positioning algorithm, probably the probabilistic one, because it can provide more variable measurements.

4.2 Filtering Result

In this section, the results of the filtering by the complementary filter to estimate the orientation, while the Kalman filter for the position. The following parts are presented by statistical evaluation and explanations towards the quality of the result, while the graphical representation is presented in appendix.

Table 4.4: Evaluation of Orientation Estimation (Azimuth) of No-Rotation Case

Smartphone	Azimuth Standard Deviation (degrees)
Wiko Highway	5.935
Samsung S4	16.136
HTC One S	1.768

Table 4.5: Evaluation of Orientation Estimation (Pitch,Roll) of No-Rotation Case

Smartphone	Averaged Absolute Error (degrees)	
	Pitch	Roll
Wiko Highway	2.116	0.703
Samsung S4	0.818	1.741
HTC One S	0.198	0.323

4.2.1 Orientation Estimation by Complementary Filter

As described in the previous chapter, the evaluation of the orientation estimation filter is based on four (4) movement tests by hand. They are no rotation, rotation in X-axis (roll), rotation in Y-axis (pitch), and rotation in Z-axis (azimuth). The three rotations are performed approximately 90°.

The quality of the filtering is measured statistically by absolute error. Absolute error evaluates how far did the measurements go from a desired value. Thus, the smaller value of absolute error means the better result.

In some cases, an angle is evaluated by standard deviation. Standard deviation is used because quality is based on the consistency to a single value which is unknown. The smaller the value of standard deviation, the estimation is more constant, which is better.

No Rotation

The smartphones were not experiencing any rotation in this case. Thus, the desired azimuth, pitch, and roll value should be constant. The pitch and roll value can be presumed as zero (0), while the azimuth cannot. It is because the azimuth is influenced by digital compass which always pointing to the digital north. Thus, the standard deviation evaluation is applied to the azimuth, while pitch and roll are evaluated by absolute error towards 0°. The graphical representation of the performance of the three smartphones is depicted by Figure B.1 in Appendix. The numerical evaluation of azimuth is presented on Table 4.4, while for pitch and roll is presented on Table 4.5.

From the graphical representation of Figure B.1, the azimuth estimation for the Samsung S4 is a little bit slower and noisier than the other two. Thus, the stability of the estimation is not good as the other two. From the numerical

Table 4.6: Evaluation of Orientation Estimation (Azimuth) of Rotation over Z-axis Case

Smartphone	Averaged Absolute Error (degrees)
Wiko Highway	22.261
Samsung S4	32.406
HTC One S	18.579

Table 4.7: Evaluation of Orientation Estimation (Pitch,Roll) of Rotation over Z-axis Case

Smartphone	Averaged Absolute Error (degrees)	
	Pitch	Roll
Wiko Highway	2.495	0.553
Samsung S4	1.034	1.281
HTC One S	0.342	0.736

evaluation presented from three table, the HTC has better sensor in the no rotation case.

Rotation over Z-axis (Azimuth)

In this case, the smartphones were experiencing approximately 90°over Z-axis in the local reference. Thus, the change of azimuth should be nearly 90°, while pitch and roll should be constant at zero (0). Then, the three angles should be evaluated by absolute error. The absolute error of azimuth is toward 90°, while, of course, pitch and roll's absolute error should be toward 0°. The graphical representation of the performance of the three smartphones is depicted by Figure B.2 in Appendix. The numerical evaluation of azimuth is presented on Table 4.6, while for pitch and roll is presented on Table 4.7.

The results for the estimation of orientation in this case is not very good. The maximum error of the azimuth change is up to 32.406°for Samsung Galaxy S4, while the minimum error is up to 18.579°by HTC One S. This is possible to happened because of the disturbance of magnetic field around the smartphone. Because the smartphone is rotated quickly, the fusion of the digital compass cannot be performed fast enough to handle the better estimation. It could be easily observed in Samsung Galaxy S4 that the change nearly 140°happened or in Wiko Highway that the estimation is noisier when the smartphone experienced the rotation rapidly. Even though so, the best estimation approach is achieved by the HTC One S.

Rotation over X-axis (Pitch)

In this case, the smartphones were experiencing approximately 90°over X-axis in the local reference. Thus, the change of pitch should be nearly 90°, while roll

Table 4.8: Evaluation of Orientation Estimation (Pitch) of Rotation over X-axis Case

Smartphone	Averaged Absolute Error (degrees)
Wiko Highway	8.008
Samsung S4	4.855
HTC One S	9.821

Table 4.9: Evaluation of Orientation Estimation (Azimuth) of Rotation over X-axis Case

Smartphone	Standard Deviation (degrees)
Wiko Highway	—
Samsung S4	—
HTC One S	8.214

should be constant at zero (0) and azimuth should be stable at unknown value. But, they might not be zero or stable at all because the surface relative to the ground of the smartphone change often. Nevertheless, the numerical evaluation will be performed those three. The absolute error of pitch change is toward 90°, while, of course, roll's absolute error should be toward 0°. The azimuth should be evaluated by standard deviation. The graphical representation of the performance of the three smartphones is depicted by Figure B.3 in Appendix. The numerical evaluation of pitch is presented on Table 4.8, while for azimuth is presented on Table 4.9 and roll is on Table 4.10. Some azimuth standard deviation evaluations cannot be presented because of some reasons which will be discussed after.

As can be seen in Figure B.3, the rotation of pitch heavily affected azimuth and slightly influenced roll. As have discussed before, it is proved that the change of the surface relative to the ground, in this case phone Z-axis to X-axis, relates to the digital compass. Hence, some observations toward the stability of the azimuth in this case were omitted because they were heavily disturbed.

Even though the measurement toward pitch might be disturbed also, but the change of the angle seemed to be indifferently not far from 90°. For those

Table 4.10: Evaluation of Orientation Estimation (Roll) of Rotation over X-axis Case

Smartphone	Averaged Absolute Error (degrees)
Wiko Highway	2.237
Samsung S4	5.818
HTC One S	4.640

Table 4.11: Evaluation of Orientation Estimation (Roll) of Rotation over Y-axis Case

Smartphone	Averaged Absolute Error (degrees)
Wiko Highway	7.182
Samsung S4	4.828
HTC One S	2.042

Table 4.12: Evaluation of Orientation Estimation (Azimuth) of Rotation over Y-axis Case

Smartphone	Standard Deviation (degrees)
Wiko Highway	2.854
Samsung S4	–
HTC One S	8.214

three smartphones, their absolute error of angle change is around 8-10 degrees. While the averaged absolute error of roll measurements were assured not to be more than 6 degrees in this experiment. Thus, it could be inferred that the filtering is good enough to handle the disturbance.

Rotation over Y-axis (Roll)

In this case, the smartphones were experiencing approximately 90°over Y-axis in the local reference. Thus, the change of roll should be nearly 90°, while pitch and azimuth should be constant at zero (0).But, they might not be zero at all because the surface relative to the ground of the smartphone change often. Nevertheless, the three angles should be evaluated by absolute error. The absolute error of roll is toward 90°, while, of course, pitch and azimuth's absolute error should be toward 0°. The graphical representation of the performance of the three smartphones is depicted by Figure B.4 in Appendix. The numerical evaluation of roll change is presented on Table 4.11, while for azimuth is presented on Table 4.12 and pitch is on Table 4.13.

Table 4.13: Evaluation of Orientation Estimation (Pitch) of Rotation over Y-axis Case

Smartphone	Averaged Absolute Error (degrees)
Wiko Highway	2.015
Samsung S4	0.583
HTC One S	4.640

As can be seen in Figure B.4, the rotation of roll affected the azimuth also, but not as much as the pitch rotation. The reason was same, the change

of the surface which relative to the ground, where in this case the change is from Z-axis to Y-axis. Hence, similar to the previous measurements, the azimuth observation of Samsung Galaxy S4 was omitted because the change was dependent to the pitch change. However, the two other smartphones' azimuth seemed not to be disturbed much about this surface change.

The overall result of this case was indifferently good, similar to the pitch change. The averaged absolute value error regarding the roll change was mostly at 7.182°by the Wiko Highway and in minimum at 2.042°by HTC One S. Thus, it can be inferred that the filter was good enough in this case.

Summary

Overall, the Complementary can estimate the orientation sufficiently good, while mostly having around single digit degrees error in best case of three smartphone. Judging from the charts, the drift which often caused by gyroscope has been successfully minimized. However, it might performed badly if there was any sudden considerable change in magnetic field around the smartphone. In future, it might be considered to have a constrain to handle this kind of sudden change for the magnetometer.

4.2.2 Position Estimation by Kalman Filter

In this part, the position estimation will be evaluated graphically and by numerical value similar to the previous orientation estimation if possible. The experiment scenario consisted of 3 movements repetitively, each movement corresponds to a single axis of smartphone's local reference. Those three movements are 15 cm right and left side of the smartphone, 15 cm forth and back, and 15 cm up and down. This scenario is performed in two approaches, the first is the usage Kalman Filter without the Wi-Fi fingerprinting result (accelerometer only) and the second is the Kalman Filter with the fusion of accelerometer and Wi-Fi fingerprinting result.

Accelerometer Only

In this part, the estimations of position of two smartphones: Wiko Highway and HTC One S will be presented. The Samsung Galaxy S4 results was not displayed because it wasn't available at the time of testing. The state estimation here is performed by using the linear acceleration (accelerometer) data. The result of the Wiko Highway is presented in Figure 4.2, while HTC One S in Figure 4.3.

From both figures of the results, it is proved that using accelerometer only didn't make any good estimation of position. This was because the sensor data from the linear acceleration were horribly noisy, which can be seen on the appendices: Figure C.1 for Wiko Highway S and Figure C.2 for HTC One S. This horrible noise might be only a small value of acceleration in the observation. But, when it was integrated two times to acquire the position

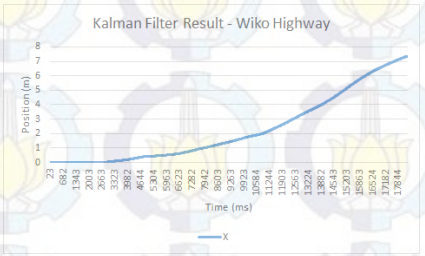

(a)

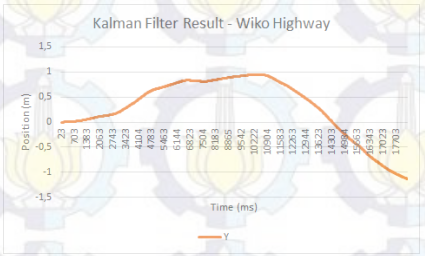

(b)

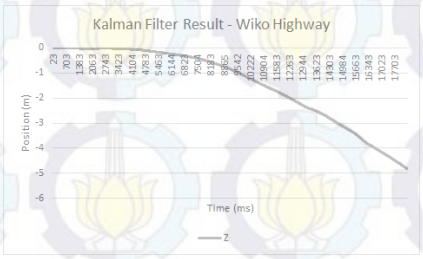

(c)

Figure 4.2: The result of position estimation in X-axis (a), Y-axis (b), and Z-axis (c) by Kalman Filter of Wiko Highway, case: using only Linear Acceleration sensor data

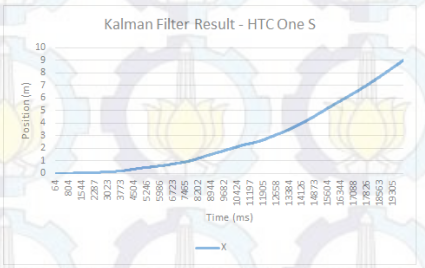

(a)

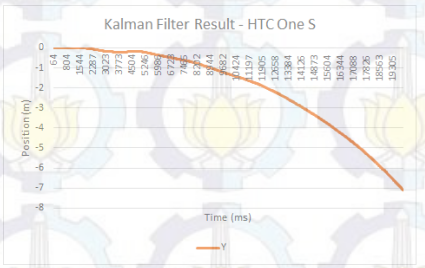

(b)

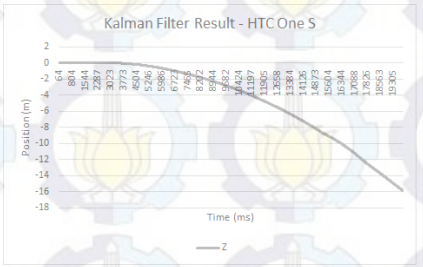

(c)

Figure 4.3: The result of position estimation in X-axis (a), Y-axis (b), and Z-axis (c) Kalman Filter of HTC One S, case: using only Linear Acceleration sensor data

estimation, the estimation wil accumulate this error value on each timestep of estimation. Hence, the error could grow into several meters in a short time.

Accelerometer with Wi-Fi Fingerprinting

In this part, the same two smartphones result of Kalman Filter using the Wi-Fi fingerprinting and linear acceleration sensor data will be presented. The results of the position estimation are presented in Figure 4.4 for the Wiko Highway S and Figure 4.5 for HTC One S.

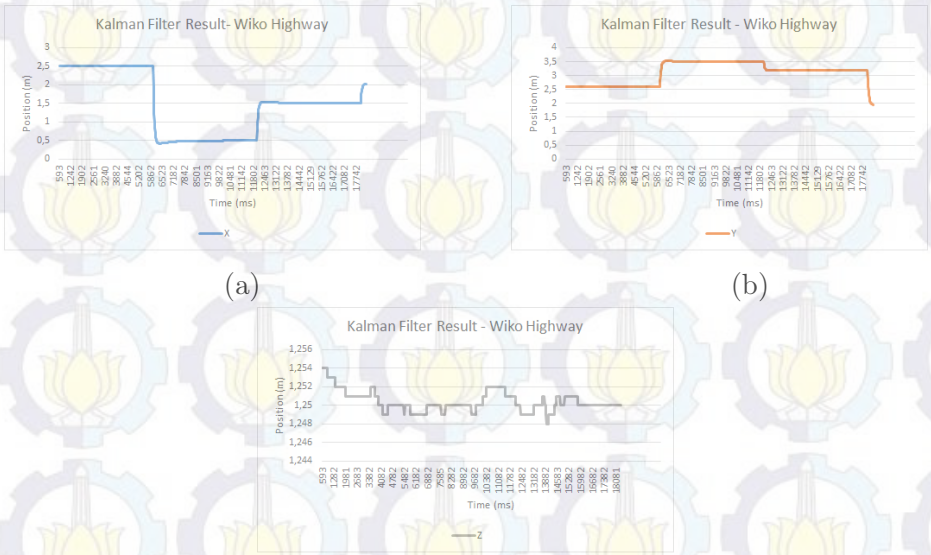

Figure 4.4: The result of position estimation in X-axis (a), Y-axis (b), and Z-axis (c) Kalman Filter of Wiko Highway, case: using only Linear Acceleration sensor data

From Figure 4.4, we can see that Wi-Fi positioning affected the position estimation heavily. The result of Wi-Fi fingerprinting give an inaccurate position toward the smartphone position when the smartphone moved. When the smartphone only moved about 15 cm, the Wi-Fi fingerprinting resulted in a jump of 3 m or no movements at all.

Hence, it was still far from accurate. The movement in all the three axis is merely about 15 cm, but the 3D position estimation was not good enough to achieve that precision. The influence of the linear acceleration existed also, but not too visible. The most notable contribution by the linear acceleration can be seen in the Z-axis position estimation subfigure, because the fingerprinting method only took a single value of Z (1.25 m) in the offline phase. In the Z-axis position estimation, the fluctuation was only about a few milimeters, which is nearly 100 times smaller than actual movement of 15 cm. In the larger scale error of other estimation, for example in the X-axis or Y-axis, this influence of the acceleration cannot be seen because of the bigger effect of the Wi-Fi fingerprinting. The more detailed observation data can be seen in appendix: Figure C.3 for the linear acceleration and Figure C.4 for the Wi-Fi positioning.

Figure 4.5: The result of position estimation in X-axis (a), Y-axis (b), and Z-axis (c) Kalman Filter of HTC One S, case: using only Linear Acceleration sensor data

From Figure 4.5, similar to the result from Wiko Highway, HTC One S position estimation also experienced the same heavy influence from Wi-Fi positioning observation. And, indeed, it was also far from accurate. Even though so, a better estimation in Z-axis than the Wiko Highway was presented there. It can be inferred from the estimation that the smartphone moved up by 1 cm, then moved back at the same position given some delays, and descends by 2 cm, then moved back again at the same position. However, it was still far from the desired outcome. The more detailed observation data can be seen in appendix: Figure C.5 for the linear acceleration and Figure C.6 for the Wi-Fi positioning.

Summary

By the two approaches of each smartphone, it can be concluded that both the options of using accelerometer only and the fusion of accelerometer and Wi-Fi fingerprinting result were not sufficient to produce good estimation of position of a smartphone. The accelerometer observation cannot give stable acceleration, while the Wi-Fi fingerprinting give far measurement from actual position. Thus, the movement of smartphone by hand, which is necessarily have to be precise up until the centimeter precision, cannot be observable using this method.

4.3 Object Pointing by Smartphone

Initially, the proposed method to evaluate both estimation of position and orientation is by moving the smartphone to desired position while rotating it to a designated object. This scenario needs the two estimation to be worked simultaneously and yields precise results. However, because of the insufficient result of position estimation, this scenario is modified.

The new proposed scenario is an object pointing scenario without position estimation. This scenario counted heavily on the orientation estimation while minimizing movement of the smartphone to point at several objects. Thus, the position of the smartphone must be as stable as possible, if not, the rotation when pointing an object would be slightly slanted and become imprecise because of difference in position.

The new scenario is composed of two different parts with different aims. The aim of the first part is to assure that the orientation estimation is stable after several random rotations. The aim of the second part is to measure the orientation estimation of the smartphone is approximately correct mathematically. The details of those two scenarios will be explained after.

The similarity of these two scenarios is the starting point. The smartphone will be hold by hand at a fixed position. Then, aided by a laser pointer attached to the smartphone, the smartphone will be rotated around to point at a desired object. The desired objects are presented in Figure 4.6 for the first scenario and Figure 4.7 for second scenario.

(a) (b)

Figure 4.6: The objects for field evaluation: first scenario

4.3.1 Object Pointing Scenario 1

After pointing at an object, the smartphone and the laser pointer will be hold as stable as possible in that position and orientation for more than 5 seconds. Afterwards, the smartphone will be moved and rotated randomly as much as possible for several seconds. Next, the smartphone will be returned in the same position and orientation as close as possible as previous when pointing at the same object. Finally, the smartphone will be held again for more than 5 seconds. To get the closest value of the orientation estimation before and

Figure 4.7: Object for the field evaluation: second scenario

after movement, the values of orientation of the predescribed 5 seconds will be averaged. This way, the orientation before and after movement should be approximately equal. Thus, the quality of the orientation estimation when pointing an object can be assured.

The evaluation for object (a) and (b) are depicted in Figure 4.8 and Figure 4.9 respectively, and summarized in Table 4.14. It can be seen in the both figures, the estimations of orientation in the end were changing into values similar to the beginning after several intentional rotations. However, as calculated mathematically, it seemed that the estimation values between the beginning and the end has error around 10 degrees, which can be inferred has around 35 cm error if the object is placed 2 m away from the smartphone. This might be happened because inconsistency of hand when holding the smartphone (human error) or the error from the estimation itself, which could be the disturbance of magnetic field.

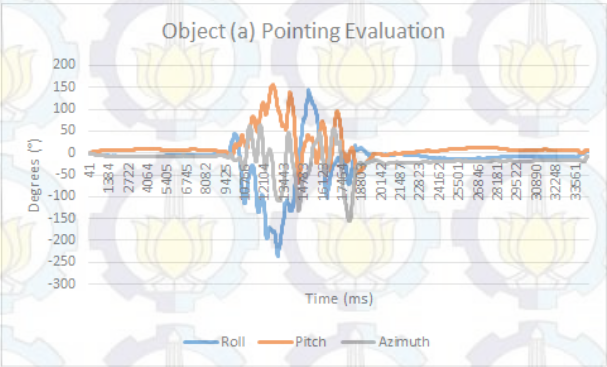

Figure 4.8: Orientation Estimation in pointing object (a) of Scenario 1

4.3.2 Object Pointing Scenario 2

The next step is a little bit different from the previous scenario. From the starting point, the smartphone will be held for more than 5 seconds. Then, the smartphone will be rotated along the local reference axes, most probably the azimuth and the pitch. Then, after the smartphone points to the desired object, it will be held for more than 5 seconds. Those 5 second time range is

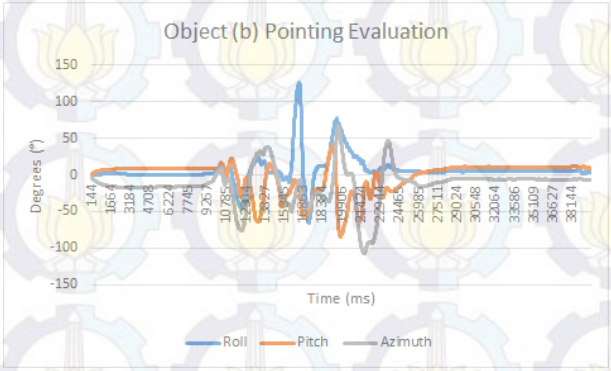

Figure 4.9: Orientation Estimation in pointing object (b) of Scenario 1

Table 4.14: Evaluation of Orientation Estimation in Pointing Object of Scenario 1

Smartphone	Estimated Angle (degrees)					
	Roll		Pitch		Azimuth	
	Beginning	End	Beginning	End	Beginning	End
Object A	−6.392	−11.380	7.477	9.204	−7.821	−18.629
Object B	0.559	5.012	8.386	10.828	−16.529	−5.771

to make sure the estimation have reached the stable orientation and to wipe out the possible noise by averaging. Note that the position of the object is also fixed and have been determined before.

By the fixed position of the smartphone and the object, the angle of the rotation can be calculated mathematically. Then, the quality of the estimation will be measured by the orientation change of the angles. These changes of angles should be approximately equal to the calculated mathematical rotation.

The object of this test only differs in the height compared with the smartphone position. Thus, the angle which should be different is the pitch. So, the only considered rotating angle in this test is the pitch. So, the pitch difference between the beginning and the end of the orientation estimation will be compared with the actual angle between the smartphone and the object. The sequences of the orientation estimation is depicted in Figure 4.10 and the angle comparison is summarized in Table 4.15.

Table 4.15: Evaluation of Orientation Estimation in Pointing Object of Scenario 1

Smartphone	Pitch angle (degrees)		
	Estimated Difference	Actual Difference	Error
Object A	16.002	15.255	**0.747**

From the result of Table 4.15, the estimation performed nicely by only leav-

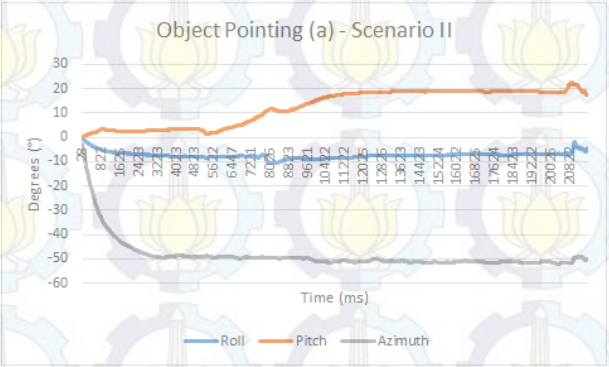

Figure 4.10: Orientation Estimation in pointing object of Scenario 2

ing 0.747°difference. In this aspect, in can be concluded that the orientation estimation gave good impression in locating object compared with mathematical computation.

4.3.3 Summary

To sum up, in the real field test, the estimation of orientation at fixed position worked sufficiently to locate some objects. But, still, there are several errors in consistency that should be taken into account because of the disturbance of hand or the magnetic field. However, it was still considerably dependable by mathematical evaluation in the case of pitch change.

[This page is intentionally left blank]

Chapter 5

Conclusion

In this chapter, a new study to approach to estimate both 3D position and orientation using the fusion of sensors of smartphone has been presented. The foreseen application of this study is to use the smartphone as a pointing device to detect interesting object inside a room. The fusion is considered because of the noisy and erroneous sensor raw data, thus the sensors alone would not be sufficient to produce adequate estimation of indoor positioning. Moreover, the desired accuracy of the positioning should be as precise as possible, and the errors of position should be in centimeter range. The proposed method is using the Complementary Filter and Kalman Filter to estimate the orientation and position respectively. To aid the position estimation, Wi-Fi fingerprinting is assigned as the observation for the position, even though it couldn't reach an accuracy as close to centimeter precision. To define how good the estimations are, the stability of the filters are measured first through simple rotations and movements. After that, the smartphones will be used to point several objects in a room for the field test.

From the 4 cases in the orientation estimation evaluation, the complementary filter showed that it could minimize the errors which produced by the gyroscope and the digital compass (magnetometer and gravity, which is derived from accelerometer). However, the error was only can be reduced into one-digit value statistically for each smartphone. Thus, this quality of estimation might draw some problem in the field test.

Unfortunately, the Kalman Filter, even by the aid of Wi-Fi, didn't perform well enough. The position estimation of Kalman filter resulted in the position error because of the Wi-Fi fingerprinting impact. The estimation only succeeded in estimating position regarding available RSSI signal. Even though small movements were detected and estimated, the position still returned to observed position from the Wi-Fi. Position estimation using Kalman Filter without Wi-Fi fingerprinting result had also been performed. But, the results became terrible because of the double integration error from the acceleration. The noise from the accelerometer-derived linear acceleration was the cause of position error until several meters as if the smartphone was not moving at all. Consequently, the estimation didn't show any meaningful result when the smartphone was moved in the range of several centimeters.

Thus, the field test scenario were adapted to only measure the quality of the orientation estimation. The field test result proved that the estimation for the orientation was slightly stable enough and mathemtically adequate to point at an object. Hence, it was feasible to use smartphone as a pointing object in when the user stood at correct position.

This study only concentrates on using the Complementary Filter and Kalman Filter within the Inertial Navigation System (INS) sensors of the smartphone plus the Wi-Fi fingerprinting. The result of this study might be different by several modifications and using other methods. It might be considerable to use additional sensors such as bluetooth or light radar to refine the precision of the estimation. However, it should be considered also about how the smartphone can handle all the sensors provided. Similar to the additional observations, the estimation methods might be modified as well. Several methods such as Wi-Fi triangulation, Particle Filters, and some variations of Kalman Filter can be counted also to do the estimation. Yet, conditions of the smartphone such as battery and the computation power should be seen as parameters to be compensated. But, it might be feasible to do these modification as the smartphone development continues to be more sophisticated.

Bibliography

[1] U. Shala and A. Rodriguez, "Indoor positioning using sensor-fusion in android devices," 2011.

[2] O. J. Woodman, "An introduction to inertial navigation," *University of Cambridge, Computer Laboratory, Tech. Rep. UCAMCL-TR-696*, vol. 14, p. 15, 2007.

[3] J. Doscher and M. Evangelist, "Accelerometer design and applications," *Analog Devices*, vol. 3, 1998.

[4] "Ieee standard specification format guide and test procedure for coriolis vibratory gyros," *IEEE Std 1431-2004*, pp. 1–78, Dec 2004.

[5] D. Hovde, M. Prouty, I. Hrvoic, and R. Slocum, "Commercial magnetometers and their application," *Optical Magnetometry*, p. 387, 2013.

[6] T. Ozyagcilar, "Implementing a tilt-compensated ecompass using accelerometer and magnetometer sensors," *Freescale semiconductor, AN*, vol. 4248, 2012.

[7] S. Ayub, A. Bahraminisaab, and B. Honary, "A sensor fusion method for smart phone orientation estimation," in *Proceedings of the 13th Annual Post Graduate Symposium on the Convergence of Telecommunications, Networking and Broadcasting, Liverpool*, 2012.

[8] B. Ando, S. Baglio, C. O. Lombardo, and V. Marletta, "An advanced tracking solution fully based on native sensing features of smartphone," in *Sensors Applications Symposium (SAS), 2014 IEEE*. IEEE, 2014, pp. 141–144.

[9] G. Welch and G. Bishop, "An introduction to the kalman filter," Chapel Hill, NC, USA, Tech. Rep., 1995.

[10] O. Costilla-Reyes and K. Namuduri, "Dynamic wi-fi fingerprinting indoor positioning system," in *International Conference on Indoor Positioning and Indoor Navigation*, vol. 27, 2014, p. 30th.

[11] Z. Chen, H. Zou, H. Jiang, Q. Zhu, Y. C. Soh, and L. Xie, "Fusion of wifi, smartphone sensors and landmarks using the kalman filter for indoor localization," *Sensors*, vol. 15, no. 1, pp. 715–732, 2015.

[12] W. Kang, S. Nam, Y. Han, and S. Lee, "Improved heading estimation for smartphone-based indoor positioning systems," in *Personal Indoor and Mobile Radio Communications (PIMRC), 2012 IEEE 23rd International Symposium on*, Sept 2012, pp. 2449–2453.

[13] C. Huang, G. Zhang, Z. Jiang, C. Li, Y. Wang, and X. Wang, "Smartphone-based indoor position and orientation tracking fusing inertial and magnetic sensing," in *Wireless Personal Multimedia Communications (WPMC), 2014 International Symposium on*, Sept 2014, pp. 215–220.

[14] N. Kothari, B. Kannan, and M. B. Dias, "Robust indoor localization on a commercial smart-phone," 2011.

[15] "Sensor manager | android developers." [Online]. Available: http://developer.android.com/reference/android/hardware/SensorManager.html

[16] "Sensors motion | android developers." [Online]. Available: http://developer.android.com/guide/topics/sensors/sensors_motion.html

[17] W. Elmenreich, "Sensor fusion in time-triggered systems," 2002.

[18] B. Li, J. Salter, A. G. Dempster, and C. Rizos, "Indoor positioning techniques based on wireless lan," in *LAN, First IEEE International Conference on Wireless Broadband and Ultra Wideband Communications*. Citeseer, 2006.

[19] R. E. Kalman, "A new approach to linear filtering and prediction problems," *Journal of Fluids Engineering*, vol. 82, no. 1, pp. 35–45, 1960.

[20] S. Colton and F. Mentor, "The balance filter," *Presentation, Massachusetts Institute of Technology*, 2007.

Appendix A

Wi-Fi RSSI Capture Sample

Table A.1: Captured RSSI by Wiko Highway S (sample)

Position (x,y,z)	Access Points						
	AP_1	AP_2	AP_3	AP_4	AP_5	AP_6	AP_7
p_A(0.5,0.5,1.25)	0	-86	-80	-65	-79	-72	-65
p_B(3,0.5,1.25)	-88	-88	-77	-62	-69	-69	-80
p_C(5.5,0.5,1.25)	-85	-84	-67	-65	-66	-67	-65
p_D(0.5,2,1.25)	0	-86	-64	-65	-65	-64	-65
p_E(3,2,1.25)	0	-86	-69	-69	-73	-68	-69
p_F(3,2,1.25)	0	-86	-75	-69	-79	-75	-69
p_G(0.5,3.5,1.25)	-86	-86	-66	-69	-67	-67	-68
p_H(3,3.5,1.25)	-86	-86	-60	-67	-59	-59	-67
p_I(3,3.5,1.25)	-86	-86	-77	-68	-77	-76	-68
p_J(0.5,5,1.25)	-86	-86	-67	-66	-71	-71	-66
p_K(3.5,1.25)	-86	-86	-65	-67	-62	-66	-72
p_L(3,5,1.25)	-86	-86	-69	-74	-67	-71	-73

Table A.2: Captured RSSI by Samsung Galaxy S4 (sample)

Position (x,y,z)	Access Points						
	AP_1	AP_2	AP_3	AP_4	AP_5	AP_6	AP_7
p_A(0.5,0.5,1.25)	-89	-83	-89	-86	-80	-89	-89
p_B(3,0.5,1.25)	-89	-86	-89	-86	-76	-89	-89
p_C(5.5,0.5,1.25)	-89	-86	-89	-86	-79	-89	-89
p_D(0.5,2,1.25)	-89	-86	-89	-86	-80	-86	-89
p_E(3,2,1.25)	-89	-86	-89	-86	-75	-89	-89
p_F(3,2,1.25)	-89	-89	-89	-86	-78	-89	-89
p_G(0.5,3.5,1.25)	-89	-89	-89	-86	-71	-89	-86
p_H(3,3.5,1.25)	-89	-86	-89	-86	-77	-89	-89
p_I(3,3.5,1.25)	-89	-89	-89	-86	-73	-89	-86
p_J(0.5,5,1.25)	-89	-89	-89	-86	-71	-89	-86
p_K(3.5,1.25)	-89	-89	-89	-86	-74	-89	-89
p_L(3,5,1.25)	-89	-83	-89	-86	-74	-89	-86

Table A.3: Captured RSSI by HTC One S (sample)

Position (x,y,z)	Access Points						
	AP_1	AP_2	AP_3	AP_4	AP_5	AP_6	AP_7
p_A(0.5,0.5,1.25)	-72	-66	-72	-72	-72	-72	-67
p_B(3,0.5,1.25)	-70	-59	-71	-71	-72	-71	-59
p_C(5.5,0.5,1.25)	-71	-72	-71	-75	-80	-77	-72
p_D(0.5,2,1.25)	-76	-63	-75	-76	-77	-76	-63
p_E(3,2,1.25)	-65	-73	-65	-63	-66	-64	-73
p_F(3,2,1.25)	-65	-62	-67	-65	-66	-65	-63
p_G(0.5,3.5,1.25)	-68	-72	-69	-67	-67	-67	-73
p_H(3,3.5,1.25)	-66	-71	-65	-65	-65	-65	-71
p_I(3,3.5,1.25)	-73	-66	-73	-72	-74	-73	-66
p_J(0.5,5,1.25)	-65	-65	-63	-63	-63	-63	-66
p_K(3,5,1.25)	-82	-76	-85	-83	-83	-82	-76
p_L(3,5,1.25)	-61	-72	-63	-62	-62	-61	-72

Appendix B

Complementary Filter Result

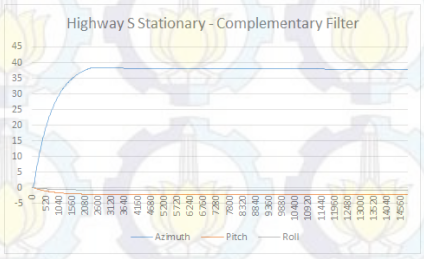

(a)

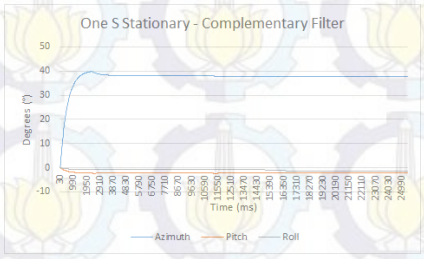

(b)

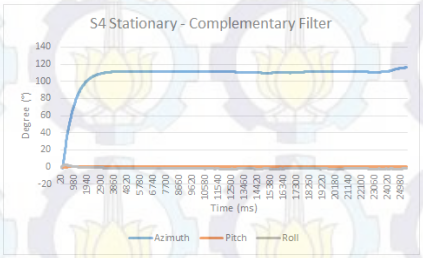

(c)

Figure B.1: The result of Complementary Filter, case: No rotation (a) Wiko Highway (b) HTC One S (c) Samsung Galaxy S4

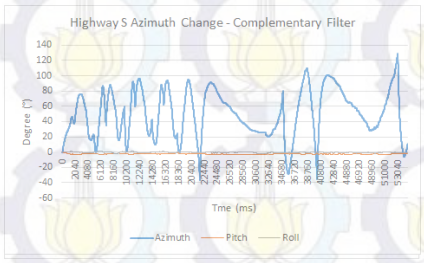

(a)

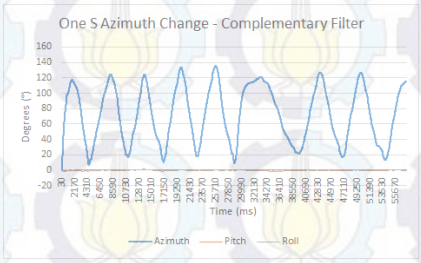

(b)

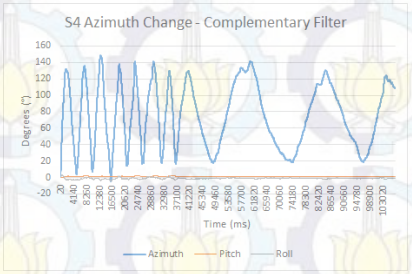

(c)

Figure B.2: The result of Complementary Filter, case: 90° Rotation over Z-axis (a) Wiko Highway (b) HTC One S (c) Samsung Galaxy S4

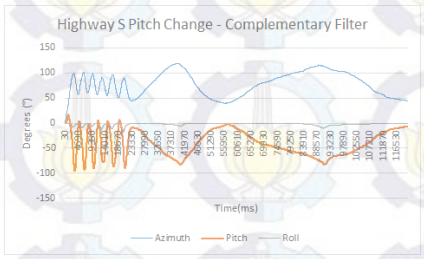

(a)

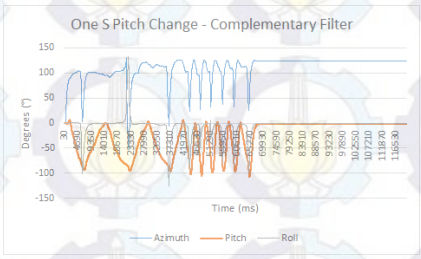

(b)

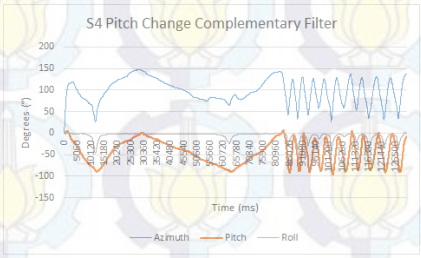

(c)

Figure B.3: The result of Complementary Filter, case: 90° Rotation over X-axis (a) Wiko Highway (b) HTC One S (c) Samsung Galaxy S4

[This page is intentionally left blank]

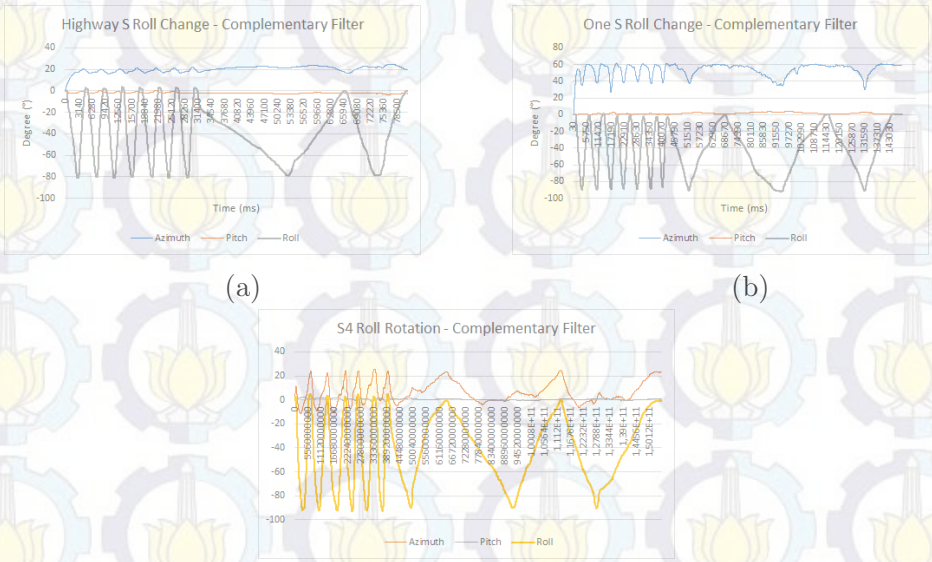

(a) (b)

(c)

Figure B.4: The result of Complementary Filter, case: 90° Rotation over Y-axis (a) Wiko Highway (b) HTC One S (c) Samsung Galaxy S4

Appendix C

Kalman Filter Observation Data

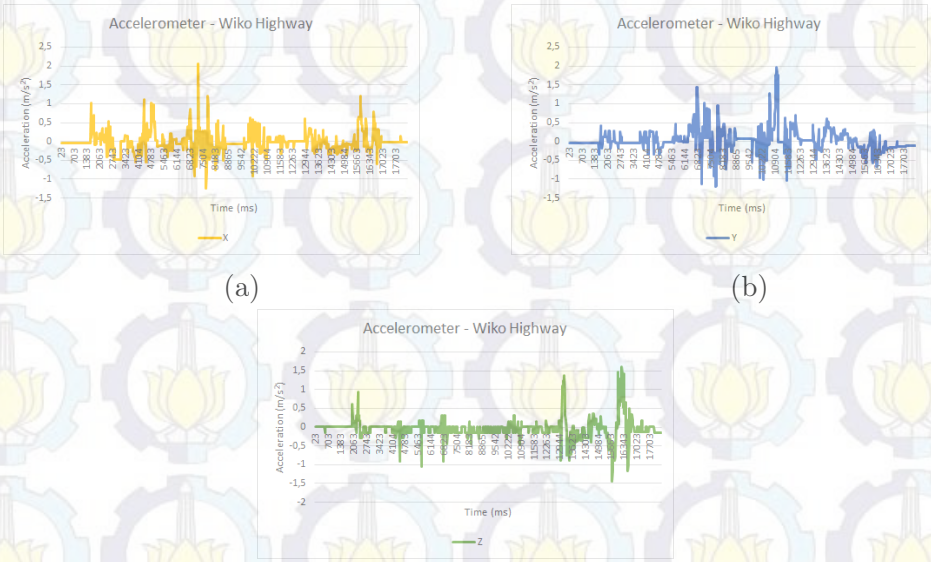

(a) (b)

(c)

Figure C.1: The linear acceleration observation of Kalman Filter of Wiko Highway in X-axis (a), Y-axis (b), and Z-axis (c), case: using only Linear Acceleration sensor data

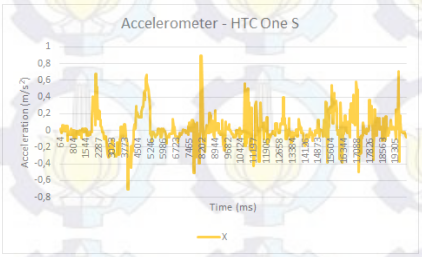

(a)

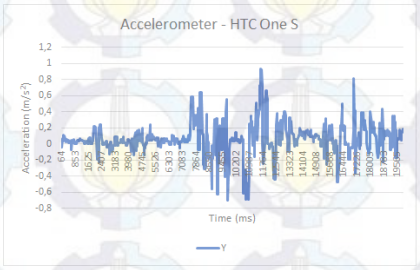

(b)

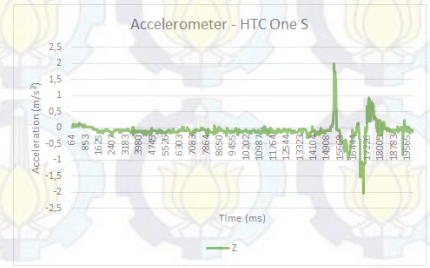

(c)

Figure C.2: The linear acceleration observation of Kalman Filter of HTC One S in X-axis (a), Y-axis (b), and Z-axis (c), case: using only Linear Acceleration sensor data

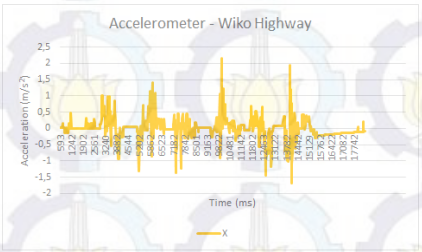

(a)

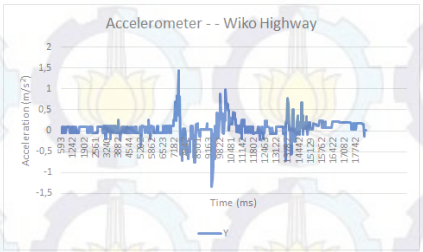

(b)

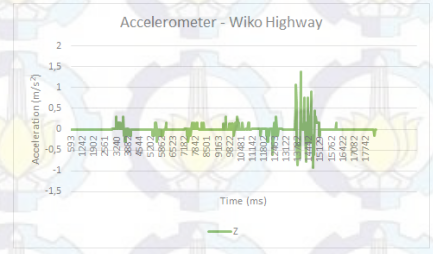

(c)

Figure C.3: The linear acceleration observation of Kalman Filter of Wiko Highway in X-axis (a), Y-axis (b), and Z-axis (c), case: fusion of Linear Acceleration sensor data and Wi-Fi fingerprinting result

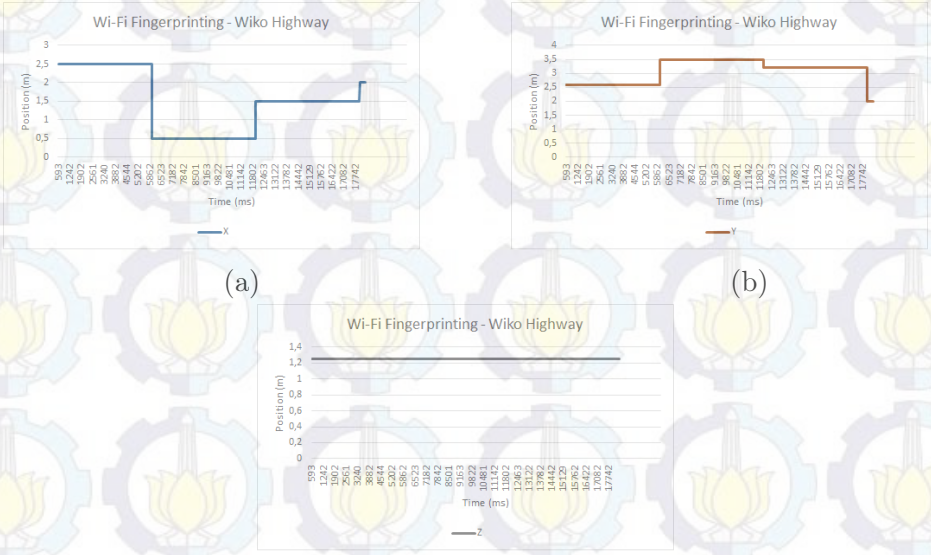

Figure C.4: The Wi-Fi positioning result observation of Kalman Filter of Wiko Highway in X-axis (a), Y-axis (b), and Z-axis (c), case: fusion of Linear Acceleration sensor data and Wi-Fi fingerprinting result

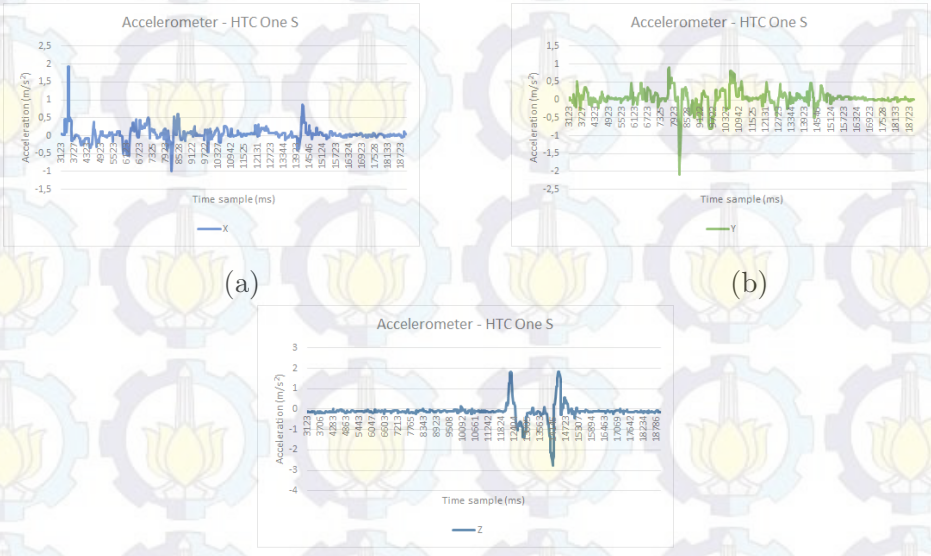

Figure C.5: The linear acceleration observation of Kalman Filter of HTC One S in X-axis (a), Y-axis (b), and Z-axis (c), case: fusion of Linear Acceleration sensor data and Wi-Fi fingerprinting result

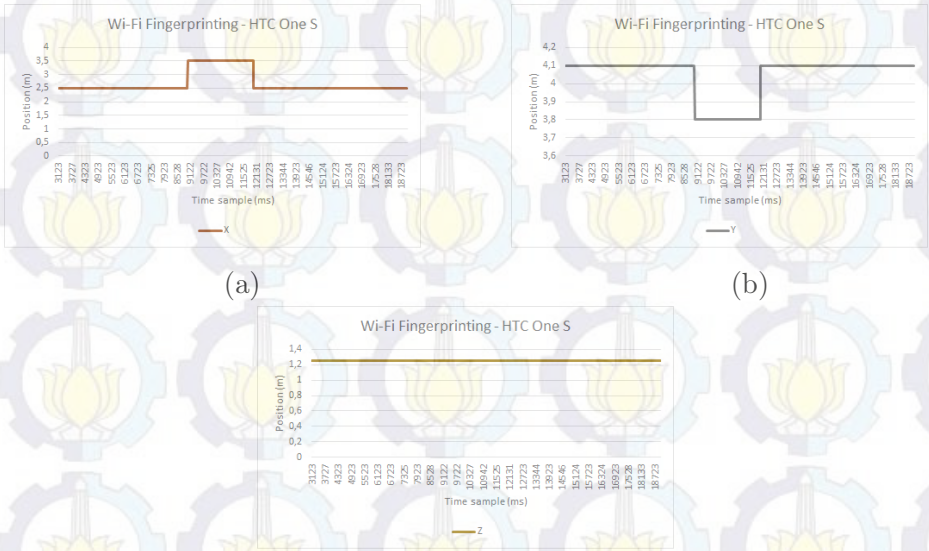

Figure C.6: The Wi-Fi positioning result observation of Kalman Filter of HTC One S in X-axis (a), Y-axis (b), and Z-axis (c), case: fusion of Linear Acceleration sensor data and Wi-Fi fingerprinting result